7-11-2013

Spin Dynamics of Trimers on a Distorted Kagome Lattice

A. Brooks Harris
University of Pennsylvania, harris@sas.upenn.edu

Taner Yildirim
University of Pennsylvania, taner@seas.upenn.edu

Recommended Citation
Harris, A., & Yildirim, T. (2013). Spin Dynamics of Trimers on a Distorted Kagome Lattice. *Physical Review B, 88* 014411-1-014411-18. http://dx.doi.org/10.1103/PhysRevB.88.014411

Spin Dynamics of Trimers on a Distorted Kagome Lattice

Abstract
We treat the ground state, elementary excitations, and neutron scattering cross section for a system of trimers consisting of three tightly bound spins 1/2 on a distorted kagome lattice, subject to isotropic nearest-neighbor (usually antiferromagnetic) Heisenberg interactions. The interactions between trimers are assumed to be weak compared to the intratrimer interactions. We compare the spin-wave excitation spectrum of trimers with that obtained from standard spin-wave theory and attribute the differences at low energy to the fact that the trimer formulation includes exactly the effects of intratrimer zero-point motion.

Disciplines
Physics | Quantum Physics

Spin dynamics of trimers on a distorted kagome lattice

A. B. Harris[1] and T. Yildirim[2,3]

[1]*Department of Physics and Astronomy, University of Pennsylvania, Philadelphia, Pennsylvania 19104, USA*
[2]*NIST Center for Neutron Research, National Institute of Science and Technology, Gaithersburg, Maryland 20899, USA*
[3]*Department of Materials Science and Engineering, University of Pennsylvania, Philadelphia, Pennsylvania 19104, USA*

(Received 3 March 2013; published 11 July 2013)

We treat the ground state, elementary excitations, and neutron scattering cross section for a system of trimers consisting of three tightly bound spins $\frac{1}{2}$ on a distorted kagome lattice, subject to isotropic nearest-neighbor (usually antiferromagnetic) Heisenberg interactions. The interactions between trimers are assumed to be weak compared to the intratrimer interactions. We compare the spin-wave excitation spectrum of trimers with that obtained from standard spin-wave theory and attribute the differences at low energy to the fact that the trimer formulation includes exactly the effects of intratrimer zero-point motion.

DOI: 10.1103/PhysRevB.88.014411 PACS number(s): 75.10.Jm, 75.25.−j, 28.20.Cz

I. INTRODUCTION

Frustrated antiferromagnetic systems have received enormous attention in recent years.[1–3] One limit which has attracted less attention is that when the frustration is removed by the formation of strongly coupled three-spin units called spin trimers.[4–10] Early experiments and calculations were performed for high ($S = \frac{5}{2}$) spin states of Fe^{3+} and Mn^{2+} by Falk *et al.*[6] and Furrer and Güdel.[5] For $S = \frac{1}{2}$ systems, much work has been focused on chainlike systems consisting of trimers of Cu ions.[4,9,10] Other configurations of trimers were studied by Qiu *et al.*[7] and Podlesnyak *et al.*[8] In these works, the interactions between trimers were very weak, so that the energy of the localized excitations appeared not to depend on wave vector. In that case, information on the nature of the excited states of the trimers was obtained by monitoring the dependence of the magnitude of the inelastic scattering cross section on wave vector. In contrast, here we will consider a system of interacting spin-$\frac{1}{2}$ trimers where the interactions between trimers is stronger, in which case the excitations have a significant dependence on wave vector. We implement perturbation theory by introducing operators which create or destroy the the exact excited states of isolated trimers. In the limit when the intertrimer interactions vanish, our calculation reduces to that of Refs. 6 and 7.

The system of trimers of spins $\frac{1}{2}$ we consider is specified by Fig. 1 where we show the covering of a distorted kagome lattice by trimers. The lattice has the connectivity of a kagome lattice, but lacks its threefold symmetry, so that the nearest-neighbor isotropic exchange interactions assume three values J, j, and k, of which J is assumed to be dominant. This model is inspired by the distorted kagome system $Cu_2(OD)_3Cl$.[11–14] The aim of this paper is to develop a calculation which is correct to leading order in j/J and k/J and to compare results obtained in this approximation to standard spin-wave theory, based on the Néel state which treats all the exchange interactions on an equal footing. We find that there is a one-to-one mapping connecting the lowest-energy manifold of excitations in the two approaches and that the differences in energies can be understood in terms of the differing way quantum zero-point motion is treated in the two approaches. At higher energy, the comparison is more complicated. In the trimer approach, one does have the higher-energy transverse spin waves of the Néel state. But in addition, some of the higher-energy trimer excitations correspond to bound states of two or more Néel-state spin excitations. The trimer approach is clearly superior when the intertrimer interactions are perturbative, as we assume in this paper.

For $Cu_2(OD)_3Cl$, a first-principles calculation[12] based in the published atomic positions[15] gave $j/J = 0.35$ and $k/J = 0.46$. However, since these values are probably too large for our perturbative approach to be valid, and since, as will become apparent, it seems to be impractical to carry our calculation to higher order, we will illustrate our results for much smaller values of these parameters. We hope that our results will stimulate the search for systems for which the ratios of the intertrimer interactions to the intratrimer interaction are smaller than for $Cu_2(OD)_3Cl$, but larger than for the systems mentioned above, in which case the results of this paper would be highly relevant. Although the results obviously depend on the details of the lattice structure, many qualitative features are robust. In particular, these systems are unusual in that although the spin configuration is collinear, in addition to the usual transverse spin-wave excitations, this system displays well-defined longitudinal (and multispin) elementary excitations which exist for all wave vectors.

Briefly, this paper is organized as follows. In Sec. II, we give a qualitative overview of the calculation in which the intertrimer interactions j and k are treated perturbatively with respect to the strong intratrimer interaction J. In Sec. III, we show that the low-energy manifold of spin waves can be mapped onto the usual manifold of spin waves, but with an effective trimer-trimer interaction playing the role of the usual spin-spin interaction. Here and in succeeding sections, we treat the two cases when (a) the net spins of adjacent trimers are coupled antiferromagnetically and (b) the net spins of adjacent trimers are coupled ferromagnetically. In Sec. IV, we consider the exciton spectrum in which trimers are promoted into their nearly localized excited states. In Sec. V, we present results of standard spin-wave calculations based on the Néel state in which all spins in the ground state have $S_z = \frac{1}{2}$ or $S_z = -\frac{1}{2}$. In Sec. VI, we compare the results the spin-wave and perturbative approaches give for the elastic diffraction pattern. We attribute the differences in results to the differences in how quantum zero-point motion is treated in the two approaches.

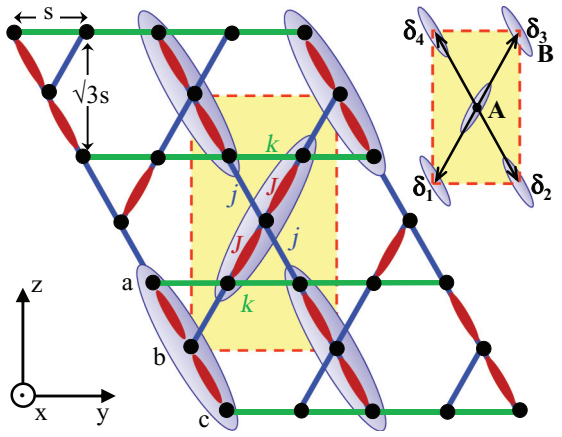

FIG. 1. (Color online) A distorted kagome lattice with three isotropic nearest-neighbor Heisenberg interactions: J (red), j (blue), and k (green). We assume J is antiferromagnetic and much larger than j and k, yielding spin trimers (some of which are shown as ellipses) which consist of three spins connected by two large interactions J. The dashed rectangle is the unit cell containing two trimers A and B. The upper right inset shows the four nearest-neighbor vectors of the trimer lattice as given in Eq. (14). Here, s is the nearest-neighbor separation between spins on the kagome lattice. The labeling of the three sites within a trimer is a, b, c in the order of decreasing z coordinate, as shown for a trimer in the left bottom corner of the unit cell.

In Sec. VII, we consider the inelastic neutron scattering cross section from the entire spectrum of trimer excitations. Our results are summarized and briefly discussed in Sec. VIII.

II. OVERVIEW

In the magnetically disordered phase of $Cu(OD)_3Cl$ (which we take as the exemplar of our trimer model), the unit cell shown in Fig. 1 contains six Cu spin sites. In Fig. 2, we show the phase diagram of the trimer model as a function of the temperature T when J is much larger than either j or k. When T is large compared to J, the spins are essentially

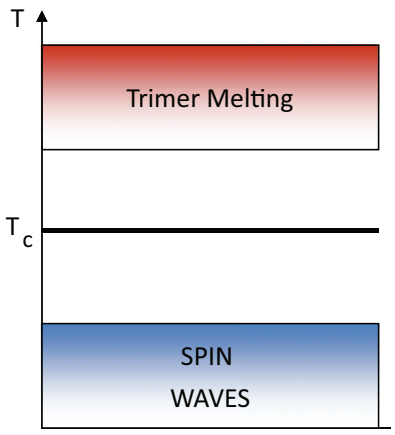

FIG. 2. (Color online) The phase diagram of the trimer system as a function of temperature T, as discussed in the text. Long-range magnetic order occurs at T_c. Trimer formation occurs over the regime for which T is of order J.

uncorrelated. As T is reduced to become comparable to J, one passes through a regime in which the correlations within spin trimers become well developed. In Fig. 2, this regime is labeled "trimer melting." Below this regime the average spin of the middle site of the trimer is oppositely oriented to those of the end sites of the trimer.[11,12] However, as long as $T > T_c$, the spin correlation function between different trimers decays rapidly as a function of their separation. When T is reduced so as to be comparable to j and/or k, one passes through a phase transition (at $T = T_c$) below which one has long-range spin order. As we discuss in the following, depending on how j and k compare, the adjacent trimers can either be organized ferromagnetically or antiferromagnetically. In either case, the magnetic ordering occurs at zero wave vector. In other words, the magnetic and paramagnetic unit cells are identical, each containing two trimer units. As we shall see, when $T \ll T_c$ the elementary excitations are identical to spin waves in the usual magnetic systems.

In contrast and as will become apparent, the higher-energy trimer excitons are qualitatively different from the higher-energy spin wave relative to the Néel ground state. To obtain a close correspondence between the two approaches, one should consider trimers consisting of three large-S spins. In that case, one should pass continuously between the trimer and Néel limits as the ratio of j or k to J is varied.

The Hamiltonian for the system of spins $\frac{1}{2}$ which we treat is written as

$$\mathcal{H} = \sum_{\langle ij \rangle} J_{ij} \mathbf{S}_i \cdot \mathbf{S}_j, \tag{1}$$

where $\langle ij \rangle$ indicates that the sum is over pairs of nearest neighbors on the kagome lattice. Here, we neglect exchange anisotropy, in particular we do not include the Dzialoshinskii-Moriya[16,17] interaction, which can be the dominant anisotropic interaction between spins.[18,19] The values of the J's are defined in Fig. 1 where the intratrimer interaction J is assumed to be dominant. We will work to leading order in j/J or k/J which are assumed to be of order $x \ll 1$. Thus, the expansion parameter x characterizes the ratio of intertrimer to intratrimer interactions. When intertrimer interactions are turned on, the spectrum of discrete energy levels of isolated trimers gets broadened into a band of wavelike excitations, just as happens for atomic energy levels when placed in a solid.

For this calculation, we obviously need the exact eigenfunctions and eigenvalues of the trimer Hamiltonian

$$\mathcal{H}_{\mathrm{T}} = J\mathbf{S}_a \cdot \mathbf{S}_b + J\mathbf{S}_b \cdot \mathbf{S}_c, \tag{2}$$

where the spins within a trimer are labeled as in Fig. 1. The total spin $\mathcal{S}$ is a good quantum number and assumes the values $\frac{3}{2}$ and $\frac{1}{2}$. The four states $\mathcal{S} = \frac{3}{2}$ are degenerate eigenstates of $\mathcal{H}_{\mathrm{T}}$ with eigenvalue $J/2$. The remaining four eigenstates form two $\mathcal{S} = \frac{1}{2}$ doublets. The eigenstates and eigenvalues of $\mathcal{H}_{\mathrm{T}}$ are listed in Table I. In the next section, we consider the ground-state manifold and in the following sections we consider excitations to the higher manifolds centered at energy J and $3J/2$ above the ground state.

Before starting the calculation, we should discuss when the trimer limit we consider is appropriate. First of all, our results show the obvious fact that when the trimers interact with one another, the single-trimer energy levels get broadened

TABLE I. Eigenvectors ψ_n and eigenvalues λ_n of $\mathcal{H}_T$. The states specified by three vertical arrows give the values of S_z for spins a, b, and c (reading from left to right), as shown in Fig. 1. The index n is only used to label excited states.

n	$\mathcal{S}$	$\mathcal{S}_z$	ψ_n	λ_n
6	$\frac{3}{2}$	$\frac{3}{2}$	$\|\uparrow,\uparrow,\uparrow\rangle$	$J/2$
5	$\frac{3}{2}$	$\frac{1}{2}$	$[\|\uparrow,\uparrow,\downarrow\rangle + \|\uparrow,\downarrow,\uparrow\rangle + \|\downarrow,\uparrow,\uparrow\rangle]/\sqrt{3}$	$J/2$
4	$\frac{3}{2}$	$-\frac{1}{2}$	$[\|\uparrow,\downarrow,\downarrow\rangle + \|\downarrow,\uparrow,\downarrow\rangle + \|\downarrow,\downarrow,\uparrow\rangle]/\sqrt{3}$	$J/2$
3	$\frac{3}{2}$	$-\frac{3}{2}$	$\|\downarrow,\downarrow,\downarrow\rangle$	$J/2$
2	$\frac{1}{2}$	$\frac{1}{2}$	$[\|\uparrow,\uparrow,\downarrow\rangle - \|\downarrow,\uparrow,\uparrow\rangle]/\sqrt{2}$	0
1	$\frac{1}{2}$	$-\frac{1}{2}$	$[\|\uparrow,\downarrow,\downarrow\rangle - \|\downarrow,\downarrow,\uparrow\rangle]/\sqrt{2}$	0
	$\frac{1}{2}$	$\frac{1}{2}$	$[\|\uparrow,\uparrow,\downarrow\rangle - 2\|\uparrow,\downarrow,\uparrow\rangle + \|\downarrow,\uparrow,\uparrow\rangle]/\sqrt{6}$	$-J$
	$\frac{1}{2}$	$-\frac{1}{2}$	$[-\|\uparrow,\downarrow,\downarrow\rangle + 2\|\downarrow,\uparrow,\downarrow\rangle - \|\downarrow,\downarrow,\uparrow\rangle]/\sqrt{6}$	$-J$

into a band. Clearly, a condition for treating isolated trimers as a starting point would be that this broadening is small enough that the bands are separated and qualitatively retain their identity from the noninteracting limit.[20] But additionally, in view of the fact that the trimers will be shown to act as spin $\frac{1}{2}$'s, one could question whether this calculation improves the treatment of quantum zero-point which can be severe for $S = \frac{1}{2}$. The following qualitative estimate indicates why the trimer calculation can be useful. Let us consider excitation relative to the Néel state in which spins are aligned along the z axis. The perturbation which creates zero-point motion comes from terms such as $J_{ij}S_-(i)S_+(j)/2$, where the subscript labels the Cartesian component of spin and the largest such terms are those for which sites i and j are *inside the same* trimer. This perturbation V connects the ground state to a state with excitation energy $E = 2zJS$, where z, the number of nearest neighbors, should be taken to be 1 or 2 because for each site there are only 1 or 2 strongly coupled neighbors. Thus, $V/E \approx \frac{1}{2}$. In contrast, when this type of calculation is repeated for the trimer state z is now 4, the number of trimer-trimer nearest neighbors. Also, perturbative corrections to a system of isolated trimers are of order $V/E = j/J$, where j is one of the intertrimer interactions. So, zero-point corrections are less important for the trimer analog of the Néel state than for the usual Néel state in the limit when j/J is small.

III. GROUND-STATE EXCITATIONS

We first consider the 2^N-fold degenerate manifold of N trimers when intertrimer interactions are turned off, so that each trimer has energy $-J$. To implement degenerate perturbation theory when intertrimer interactions are turned on, it is convenient to map this manifold of states onto the 2^N states associated with a system of N pseudospin $\frac{1}{2}$ operators, such that the pseudospin operator of each trimer is simply the total ground-state spin operators $\mathcal{S}$ of that trimer. For the trimer at position $\mathbf{R}$ we denote this pseudospin operator as $\boldsymbol{\sigma}(\mathbf{R})$. Then, any operator within the ground manifold can be expressed in terms of products of one or more $\boldsymbol{\sigma}(\mathbf{R})$. We then use the wave functions in Table I to express matrix elements of spin operators for individual sites within the trimer at $\mathbf{R}$ to $\boldsymbol{\sigma}(\mathbf{R})$. For this purpose, we label the three spins within a trimer as a, b, and c as in Fig. 1. Using Table I we note that for an A trimer (for which $\boldsymbol{\sigma}_z = \frac{1}{2}$), the expectation value of the z component of the kth spin in the ground state of the trimer denoted $S_z(k)$ (where $k = a,b,c$) is

$$S_z(a) = 1/3, \quad S_z(b) = -1/6, \quad S_z(c) = 1/3. \tag{3}$$

This result reflects the fact that the central spin partakes of spin fluctuations with its two neighbors inside the trimer whereas an end spin of the trimer has only one neighbor with which to fluctuate. Below we will discuss the experimental consequences of this result. In fact, the Wigner-Eckart theorem[21] indicates that we have, *as an operator equality within the ground manifold*, that

$$\begin{aligned} \mathbf{S}(a;\mathbf{R}) &= 2\boldsymbol{\sigma}(\mathbf{R})/3, \\ \mathbf{S}(b;\mathbf{R}) &= -\boldsymbol{\sigma}(\mathbf{R})/3, \\ \mathbf{S}(c;\mathbf{R}) &= 2\boldsymbol{\sigma}(\mathbf{R})/3, \end{aligned} \tag{4}$$

where $\mathbf{S}(k;\mathbf{R})$ is the operator for the kth spin in the trimer whose center is at $\mathbf{R}$ and, as we have said, the pseudospin operator is identified as the total spin of the trimer:

$$\boldsymbol{\sigma}(\mathbf{R}) = \sum_{k=a}^{c} \mathbf{S}(k;\mathbf{R}). \tag{5}$$

These equalities make it a trivial matter to write the intertrimer interactions in terms of the $\boldsymbol{\sigma}$'s. So we see, even without calculation, that the low-energy spectrum of the trimer system is identical to that of a system in which each trimer is replaced by an ordinary spin $\frac{1}{2}$.

We now consider the ground state and elementary excitations of the system when weak interactions between trimers are included. We will assume that all end-to-end exchange interactions between nearest-neighbor trimers assume a common value k and those between the end of one trimer and the center of its nearest neighbor assume a common value j as shown in Fig. 1. This symmetry we have imposed makes the calculations algebraically simple. If the intratrimer and intertrimer interactions have no special symmetry, the calculations become algebraically more complicated but are conceptually no more difficult. So, here we give results only for the model of Fig. 1.

We now construct the effective Hamiltonian *within the ground-state manifold.* Consider the interaction $V(A,B)$ between trimers A and B. We use the Wigner-Eckart theorem to express the spin operators in terms of the pseudospin or

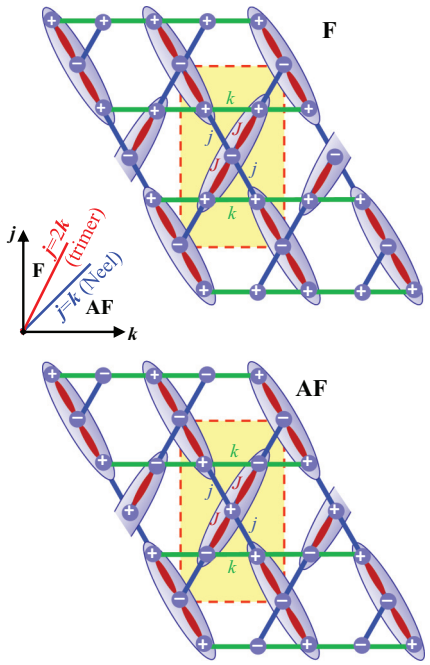

FIG. 3. (Color online) As Fig. 1, the ferromagnetic (F) and antiferromagnetic (AF) arrangement of trimers, with spin orientation indicated by + or −. The inset graph shows the phase diagram of the trimer system in the j-k plane. The F-AF phase boundary based on the Néel state is at $j = k$ and according to the trimer calculation is at $j = 2k$. The latter calculation is more nearly correct when J is large compared to j or k, whereas the former is more accurate when J is not large compared to j and k.

total spin of the trimer, as done in Eq. (4). Then, one sees that $V(A,B)$ *within the ground manifold* is given by

$$V(A,B) = [\boldsymbol{\sigma}(A)\cdot\boldsymbol{\sigma}(B)][4k-2j]/9 \equiv \mathcal{J}[\boldsymbol{\sigma}(A)\cdot\boldsymbol{\sigma}(B)], \quad (6)$$

where

$$\mathcal{J} = (4k-2j)/9. \quad (7)$$

One sees that the effective exchange interaction between two nearest-neighboring trimers is antiferromagnetic if $2k - j > 0$ and is ferromagnetic if $2k - j < 0$.[22] Thus, the trimer-trimer interaction can be ferromagnetic even if all the spin-spin interactions are positive (antiferromagnetic) providing $j > 2k$. These configurations are shown in Fig. 3. The elementary excitations within the ground manifold are those of a rectangular centered lattice. Then, if the trimers are antiferromagnetically coupled, standard spin-wave theory[23] gives the doubly degenerate spin-wave energy $\omega_{\pm}(\mathbf{q})$ as a function of wave vector $\mathbf{q}$, for $-\pi/(2s) < q_y < \pi/(2s)$ and $-\pi/(2\sqrt{3}s) < q_z < \pi/(2\sqrt{3}s)$, as

$$\omega(\mathbf{q}) = z\mathcal{J}S\sqrt{1-\gamma(\mathbf{q})^2}, \quad (8)$$

where $z = 4$ is the number of nearest neighbors, $S = \frac{1}{2}$, and

$$\gamma(\mathbf{q}) = (1/z)\sum_{\boldsymbol{\delta}} \exp(i\mathbf{q}\cdot\boldsymbol{\delta}) = \cos(sq_y)\cos(\sqrt{3}sq_z). \quad (9)$$

Here, $\boldsymbol{\delta}$ is summed over nearest-neighbor vectors between trimers and s is the nearest-neighbor separation in the kagome lattice, as in Fig. 1. If the trimers are ferromagnetically coupled, then one has two nondegenerate modes whose energy is given by

$$\omega_{\pm}(\mathbf{q}) = z|\mathcal{J}|S[1 \pm \gamma(\mathbf{q})]. \quad (10)$$

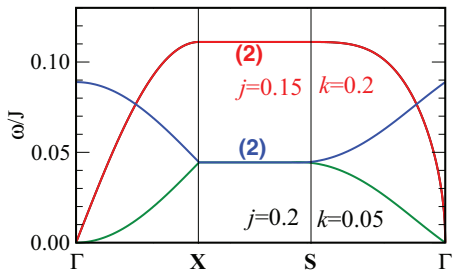

FIG. 4. (Color online) Spectrum of excitation energy $\omega(\mathbf{q})$ within the ground manifold for wave vectors in special directions. Here and below, we plot the spectra for $J = 1$ for wave vectors on the lines joining Γ and **X**, **X**, and **S**, and **S** and Γ, where $\Gamma = (0,0)$, $X = [\pi/(2s),0]$, and $S = [\pi/(2s),\pi/(2\sqrt{3}s)]$. For $(j = 0.15,\ k = 0.2)$ one has an antiferromagnetic configuration of trimers and for $(j = 0.2, k = 0.05)$ one has a ferromagnetic configuration of trimers. The modes shown here appear only in the transverse (+−) response function. Modes are nondegenerate unless labeled "(2)" to indicate a twofold degeneracy.

Here (in Fig. 4) and in the following, we give results for $J = 1$ for the antiferromagnetic configuration of trimers with $j = 0.15$ and $k = 0.2$ and for the ferromagnetic configuration with $j = 0.2$ and $k = 0.05$. Note that transverse (+−) modes of the antiferromagnetic configuration of trimers are doubly degenerate for all wave vectors. Also, here and below note that the spectrum is always twofold degenerate for wave vectors on the face of the Brillouin zone $[k_y = \pi/(2s)]$ due to the Kramers-type degeneracy from the twofold screw axis (Ref. 24).

IV. EXCITON SPECTRUM

Now we turn to the excitations out of the ground-state manifold.

A. Manifold at energy J for the antiferromagnetic configuration

Here, we treat the case of antiferromagnetic coupling ($\mathcal{J} > 0$). The situation for this manifold is more complicated than that for the ground manifold. For the ground manifold, we could develop degenerate perturbation theory for the manifold of 2^N states of the system of N trimers in which each trimer independently occupies one of its two degenerate ground states. The result was embodied in an effective Hamiltonian in which the interactions between nearest-neighboring trimers was given by Eq. (7). For excitations near energy J we might consider the manifold of states in which one trimer occupies one of the excited states of Table I and all the other $N-1$ trimers are distributed over the two degenerate ground states. Strictly speaking, this involves the solution to a many-body problem for the states of a spin excitation within the ground manifold and an exciton at excitation energy J or $3J/2$. We will not treat this system with this degree of sophistication.

Instead, we will treat the manifold of excited states at relative energy J or $3J/2$ when all the background trimers are confined to their broken symmetry ground state. Thus, our treatment is limited to the range of temperature T for which $kT \ll \mathcal{J}$. We therefore introduce operators $a_n^\dagger(\mathbf{R})$ which take the trimer at $\mathbf{R}$ from its ground state to its nth excited state, where the labeling of sites is given in the first column of Table I. The Hamiltonian which describes the manifold at energy J is

$$\mathcal{H}(J) = J \sum_{\mathbf{R}} \sum_{n=1}^{2} n_n(\mathbf{R}) + V(J), \tag{11}$$

where $\mathbf{R}$ is summed over trimer sites and $n_n = a_n^\dagger a_n$. Within the manifold near energy J, the term in Eq. (11) proportional to J is a constant and the nature of the band states is determined solely by the perturbation $V(J)$, which contains only terms proportional to j or k. To obtain results to leading order in the expansion parameter x, the perturbation $V(J)$ is thus restricted to terms which conserve the unperturbed energy J. Accordingly, the most general such form of $V(J)$ is

$$V(J) = \sum_{\mathbf{R},\mathbf{R}'} \sum_{n,m=1}^{2} c_{nm}(\mathbf{R},\mathbf{R}') a_n^\dagger(\mathbf{R}) a_m(\mathbf{R}') + \cdots, \tag{12}$$

where the ellipsis denotes terms containing p creation operators (all with indices in the range 1,2) and p analogous destruction operators with $p > 1$. Since we only consider nearest-neighbor interactions, we set

$$\mathbf{R}' = \mathbf{R}_n = \mathbf{R} + \boldsymbol{\delta}_n, \tag{13}$$

where $\boldsymbol{\delta}_n$ are the nearest-neighbor intertrimer displacements shown in Fig. 1:

$$\begin{aligned} \boldsymbol{\delta}_1 &= -s\hat{j} - \sqrt{3}s\hat{k}, \quad \boldsymbol{\delta}_2 = s\hat{j} - \sqrt{3}s\hat{k}, \\ \boldsymbol{\delta}_3 &= s\hat{j} + \sqrt{3}s\hat{k}, \quad \boldsymbol{\delta}_4 = -s\hat{j} + \sqrt{3}s\hat{k}. \end{aligned} \tag{14}$$

The effect of these $2p$th order terms in Eq. (12) on the mode energies is proportional to the $(p-1)$th power of the density of excitations. Since we assume that $kT \ll J$, this density is small and we keep only the terms with $p = 1$. In addition, we ignore the kinematic constraint which allows one to map the finite number of trimer states onto the infinite number of bosonic states.[25] The discussion for the band at energy $3J/2$ is completely analogous to that for energy J and the analogous result holds for that case. So, the band states are completely determined by the matrix $c_{n,m}(\mathbf{R},\mathbf{R}')$ or, as we shall see, by its Fourier transform which is a 4×4 matrix for the band at energy J and an 8×8 matrix for the band at energy $3J/2$. To explicitly determine $V(J)$, we must express the spin Hamiltonian in terms of the creation and annihilation operators of Eq. (12). The spin interaction between the kth spin of an up trimer at $\mathbf{R}$ and the k'th spin of a down trimer at $\mathbf{R}'$ is

$$\begin{aligned} \mathbf{S}(k;\mathbf{R}) \cdot \mathbf{S}(k';\mathbf{R}') = {} & S_z(k;\mathbf{R}) S_z(k';\mathbf{R}') + [S_+(k;\mathbf{R}) S_-(k';\mathbf{R}') \\ & + S_-(k;\mathbf{R}) S_+(k';\mathbf{R}')]/2. \end{aligned} \tag{15}$$

Since S_+ and S_- each involve at least one creation or annihilation operator, to construct the boson Hamiltonian, we need only keep terms in these operators which are linear in the creation or destruction operators. In contrast, since S_z has a nonzero value in the ground state, we also need to keep terms in S_z which involve one creation operator and one destruction operator within the band. These considerations will be used implicitly below to limit the complexity of the mapping from spins to bosons.

For the case of an "up" trimer at $\mathbf{R}$ (one whose ground state has $\mathcal{S}_z = \frac{1}{2}$ and which we refer to as an "A" trimer), we find (keeping only terms linear in the boson operators) that

$$\begin{aligned} S_-(a;\mathbf{R}) &= a_1^\dagger(\mathbf{R})/\sqrt{3} - a_4^\dagger(\mathbf{R})/\sqrt{18} + a_6(\mathbf{R})/\sqrt{6}, \\ S_-(b;\mathbf{R}) &= 2a_4^\dagger(\mathbf{R})/\sqrt{18} - 2a_6(\mathbf{R})/\sqrt{6}, \\ S_-(c;\mathbf{R}) &= -a_1^\dagger(\mathbf{R})/\sqrt{3} - a_4^\dagger(\mathbf{R})/\sqrt{18} + a_6(\mathbf{R})/\sqrt{6}. \end{aligned} \tag{16}$$

The expression for $S_+(k,\mathbf{R})$ is obtained by Hermitian conjugation. To determine the bosonic equivalent of S_z we write

$$S_z = a_0 + \sum_{nm} a_{nm} a_n^\dagger a_m. \tag{17}$$

To determine the coefficients, we require that the two representations lead to the same matrix elements. Thus, if 0 labels the ground state (i.e., whichever of the $-J$ states of the trimer is the ground state), then, by taking matrix elements of both sides of Eq. (17) we get

$$\begin{aligned} a_0 &= \langle 0|S_z|0\rangle, \quad a_{n,m} = \langle n|S_z|m\rangle, \quad n \neq m \\ a_0 + a_{n,n} &= \langle n|S_z|n\rangle, \quad n \neq 0. \end{aligned} \tag{18}$$

So, for diagonal elements we must remember to subtract off the ground-state value when identifying the bosonic matrix elements a_{nn}. Thus,

$$\begin{aligned} S_z(a;\mathbf{R}) = {} & 1/3 + a_2^\dagger(\mathbf{R})/\sqrt{12} - a_5^\dagger(\mathbf{R})/\sqrt{18} \\ & + a_2(\mathbf{R})/\sqrt{12} - a_5(\mathbf{R})/\sqrt{18} - [2n_1(\mathbf{R}) + 2n_2(\mathbf{R}) \\ & + 5n_3(\mathbf{R}) + 3n_4(\mathbf{R}) + n_5(\mathbf{R}) - n_6(\mathbf{R})]/6, \\ S_z(b;\mathbf{R}) = {} & -1/6 + 2a_5^\dagger(\mathbf{R})/\sqrt{18} \\ & + 2a_5(\mathbf{R})/\sqrt{18} - n_1(\mathbf{R})/3 + 2n_2(\mathbf{R})/3 - n_3(\mathbf{R})/3 \\ & + n_5(\mathbf{R})/3 + 2n_6(\mathbf{R})/3, \\ S_z(c;\mathbf{R}) = {} & 1/3 - a_2^\dagger(\mathbf{R})/\sqrt{12} - a_5^\dagger(\mathbf{R})/\sqrt{18} \\ & - a_2(\mathbf{R})/\sqrt{12} - a_5(\mathbf{R})/\sqrt{18} - [2n_1(\mathbf{R}) + 2n_2(\mathbf{R}) \\ & + 5n_3(\mathbf{R}) + 3n_4(\mathbf{R}) + n_5(\mathbf{R}) - n_6(\mathbf{R})]/6. \end{aligned} \tag{19}$$

Here, we needed to keep $a_p^+ a_p \equiv n_p$ terms in view of Eqs. (15) and (18).

For the case of a "down" trimer (one whose ground state has $\mathcal{S}_z = -\frac{1}{2}$ at $\mathbf{R}$ and which we refer to as a "B" trimer), we similarly find that

$$\begin{aligned} S_+(a;\mathbf{R}) &= a_2^\dagger(\mathbf{R})/\sqrt{3} + a_5^\dagger(\mathbf{R})/\sqrt{18} - a_3(\mathbf{R})/\sqrt{6}, \\ S_+(b;\mathbf{R}) &= -2a_5^\dagger(\mathbf{R})/\sqrt{18} + 2a_3(\mathbf{R})/\sqrt{6}, \\ S_+(c;\mathbf{R}) &= -a_2^\dagger(\mathbf{R})/\sqrt{3} + a_5^\dagger(\mathbf{R})/\sqrt{18} - a_3(\mathbf{R})/\sqrt{6}, \\ S_z(a;\mathbf{R}) &= -1/3 - a_1^\dagger(\mathbf{R})/\sqrt{12} - a_4^\dagger(\mathbf{R})/\sqrt{18} - a_1(\mathbf{R})/\sqrt{12} \\ & \quad - a_4(\mathbf{R})/\sqrt{18} + n_1(\mathbf{R})/3 + n_2(\mathbf{R})/3 - n_3(\mathbf{R})/6 \\ & \quad + n_4(\mathbf{R})/6 + n_5(\mathbf{R})/2 + 5n_6(\mathbf{R})/6, \end{aligned}$$

$$
\begin{aligned}
S_z(b;\mathbf{R}) &= 1/6 + 2a_4^\dagger(\mathbf{R})/\sqrt{18} \\
&\quad + 2a_4(\mathbf{R})/\sqrt{18} - 2n_1(\mathbf{R})/3 + n_2(\mathbf{R})/3 \\
&\quad - 2n_3(\mathbf{R})/3 - n_4(\mathbf{R})/3 + n_6(\mathbf{R})/3, \\
S_z(c;\mathbf{R}) &= -1/3 + a_1^\dagger(\mathbf{R})/\sqrt{12} \\
&\quad - a_4^\dagger(\mathbf{R})/\sqrt{18} + a_1(\mathbf{R})/\sqrt{12} - a_4(\mathbf{R})/\sqrt{18} \\
&\quad + n_1(\mathbf{R})/3 + n_2(\mathbf{R})/3 - n_3(\mathbf{R})/6 \\
&\quad + n_4(\mathbf{R})/6 + n_5(\mathbf{R})/2 + 5n_6(\mathbf{R})/6. \qquad (20)
\end{aligned}
$$

The next step is to write the interaction between trimers in terms of boson operators. Since we treat here the case when the trimers are antiferromagnetically coupled, all interactions couple an up (A) trimer to a down (B) trimer. Since we treat only nearest-neighbor interactions, we need consider only interactions between an up trimer at $\mathbf{R}$ and one of its four down neighbors at $\mathbf{R}\pm\boldsymbol{\delta}_1$ and $\mathbf{R}\pm\boldsymbol{\delta}_2$. For the excitations band near energy J the boson Hamiltonian is obtained in Appendix A. We define the Fourier transformed variables as

$$
\begin{aligned}
a_{n,A}^\dagger(\mathbf{k}) &= N^{-1/2}\sum_{\mathbf{R}\in A} e^{i\mathbf{k}\cdot\mathbf{R}} a_n^\dagger(\mathbf{R}), \\
a_{n,B}^\dagger(\mathbf{k}) &= N^{-1/2}\sum_{\mathbf{R}\in B} e^{i\mathbf{k}\cdot\mathbf{R}} a_n^\dagger(\mathbf{R}),
\end{aligned} \qquad (21)
$$

where N is the total number of unit cells in the system. The quadratic Hamiltonian is of the canonical form $\mathcal{H}=\sum_{\mathbf{q}}\mathcal{H}_{\mathbf{q}}$, where $\mathbf{q}$ is the wave vector and because we need consider only terms which conserve the unperturbed energy J:

$$
\mathcal{H}_{\mathbf{q}} = \sum_{n,n';\tau,\tau'} A_{st}(\mathbf{q}) a_s^\dagger(\mathbf{q}) a_t(\mathbf{q}), \qquad (22)
$$

where $s\equiv(n,\tau)$ and $t\equiv(n',\tau')$.

According to Table I, excitations near energy J involve states 1 and 2 of the two spins in the unit cell, whereas excitations near energy $3J/2$ involve states 3, 4, 5, and 6 of the two spins in the unit cell. For excitations near energy J we write

$$
\mathbf{A} = J\mathcal{I} + k\mathbf{A}_k + j\mathbf{A}_j, \qquad (23)
$$

where $\mathcal{I}$ is the 4×4 unit matrix and Eq. (A31) of Appendix A implies that

$$
\mathbf{A}_k = \frac{1}{9}\begin{bmatrix} 4 & 0 & 0 & 0 \\ 0 & 4 & 3\gamma(\mathbf{q}) & 0 \\ 0 & 3\gamma(\mathbf{q}) & 4 & 0 \\ 0 & 0 & 0 & 4 \end{bmatrix} \qquad (24)
$$

and

$$
\mathbf{A}_j = \frac{1}{9}\begin{bmatrix} 1 & 0 & 0 & 0 \\ 0 & -5 & 0 & 0 \\ 0 & 0 & -5 & 0 \\ 0 & 0 & 0 & 1 \end{bmatrix}. \qquad (25)
$$

The rows and columns of the matrices $\mathbf{A}$ are labeled in the order $(1,A)$, $(2,A)$, $(1,B)$, $(2,B)$.

Thus, the creation operators for the normal modes are $a_{1,A}(\mathbf{q})^\dagger$, $a_{2,B}(\mathbf{q})^\dagger$, and

$$
\rho_\pm^\dagger = [a_{1,B}(\mathbf{q})^\dagger \pm a_{2,A}(\mathbf{q})^\dagger]/\sqrt{2}, \qquad (26)
$$

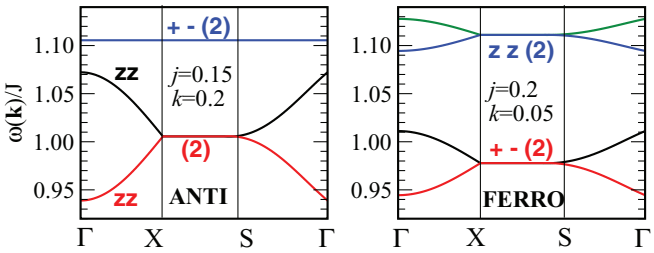

FIG. 5. (Color online) As Fig. 4, but for excitations in the manifold near energy J for the antiferromagnetic (left) and ferromagnetic (right) configurations. The curve labeled "+−" indicates the energy in the transverse (+−) response function and those labeled "zz" are the energies in the longitudinal (zz) response function. The numbers in parentheses indicate the degeneracy of the mode.

with associated eigenenergies

$$
\omega_{1A}(\mathbf{q}) = \omega_{2B}(\mathbf{q}) = J + (4k+j)/9 \qquad (27)
$$

and

$$
\omega_\pm(\mathbf{q}) = J + (4k-5j)/9 \pm (k/3)\gamma(\mathbf{q}). \qquad (28)
$$

These results are shown in Fig. 5. For an A (up) trimer $a_{1,A}^\dagger$ corresponds to S_- and $a_{2,B}^\dagger$ corresponds to S_+ for a B (down) trimer. So, these operators create transverse excitations and similarly one sees that $\rho_\pm^\dagger$ create a longitudinal excitation. It may be surprising that, unlike for a Néel antiferromagnet, the longitudinal excitations exhibit dispersion, but the transverse ones do not. However, note that for a Néel antiferromagnet, the dispersion comes from $a^\dagger a^\dagger$ terms which here are eliminated since they do not conserve the large unperturbed energy.

B. Manifold at energy J for the ferromagnetic configuration

The calculations for the ferromagnetic configuration (in which all trimers start in their "up" ground state) are similar and are done in Appendix C. In terms of Fourier transformed variables, Eq. (C31) implies, in the notation of Eq. (23), that

$$
\mathbf{A}_j = \frac{1}{9}\begin{bmatrix} -1 & 0 & 0 & 0 \\ 0 & 5 & 0 & 0 \\ 0 & 0 & -1 & 0 \\ 0 & 0 & 0 & 5 \end{bmatrix}, \qquad (29)
$$

$$
\mathbf{A}_k = \frac{1}{9}\begin{bmatrix} -4 & 0 & -6\gamma(\mathbf{q}) & 0 \\ 0 & -4 & 0 & -3\gamma(\mathbf{q}) \\ -6\gamma(\mathbf{q}) & 0 & -4 & 0 \\ 0 & -3\gamma(\mathbf{q}) & 0 & -4 \end{bmatrix}, \qquad (30)
$$

where the rows and columns are labeled in the order $(A,1)$, $(A,2)$, $(B,1)$, $(B,2)$. The eigenvalues give the mode energies

$$
\begin{aligned}
\omega_{1,2} &= J - j/9 - 4k/9 \pm 2k\gamma(\mathbf{q})/3, \\
\omega_{3,4} &= J + 5j/9 - 4k/9 \pm k\gamma(\mathbf{q})/3.
\end{aligned} \qquad (31)
$$

These mode energies are shown for high-symmetry wave vectors in Fig. 5. Since $a_{A1}^\dagger$ or $a_{B1}^\dagger$ connects the up ground state to a state with $\mathcal{S}_z=-\frac{1}{2}$, these operators correspond to an S_-. Thus, we identify $\omega_{1,2}$ as energies of transverse excitations and $\omega_{3,4}$ as energies of longitudinal excitations as indicated in Fig. 5.

C. Manifold at energy $3J/2$ for the antiferromagnetic configuration

Here, we adopt the same simplified approximation in which trimers not in excited states remain in their Néel state. Then, to leading order in the intertrimer interactions, we only keep terms which are quadratic in the variables 3, 4, 5, and 6 and which conserve the total number of excitations. Thus, analogously to Eq. (11) we write

$$\mathcal{H}(3J/2) = (3J/2)\sum_{\mathbf{R}}\sum_{n=3}^{6} n_n(\mathbf{R}) + V(3J/2). \quad (32)$$

The evaluation of $V(3J/2)$ for the antiferromagnetic configuration is given in Eq. (B38) of Appendix B. In the notation of Eq. (23), where we label the rows and columns of the matrices in the order $3A$, $6B$, $4A$, $3B$, $5A$, $4B$, $6A$, $5B$, that result implies that

$$\mathbf{A}_k = \frac{1}{9}\begin{bmatrix} 10 & 0 & 0 & 0 & 0 & 0 & 0 & 0 \\ 0 & 10 & 0 & 0 & 0 & 0 & 0 & 0 \\ 0 & 0 & 6 & X & 0 & 0 & 0 & 0 \\ 0 & 0 & X & -2 & 0 & 0 & 0 & 0 \\ 0 & 0 & 0 & 0 & 2 & Y & 0 & 0 \\ 0 & 0 & 0 & 0 & Y & 2 & 0 & 0 \\ 0 & 0 & 0 & 0 & 0 & 0 & -2 & X \\ 0 & 0 & 0 & 0 & 0 & 0 & X & 6 \end{bmatrix}, \quad (33)$$

$$\mathbf{A}_j = \frac{1}{18}\begin{bmatrix} -1 & 0 & 0 & 0 & 0 & 0 & 0 & 0 \\ 0 & -1 & 0 & 0 & 0 & 0 & 0 & 0 \\ 0 & 0 & -3 & T & 0 & 0 & 0 & 0 \\ 0 & 0 & T & -7 & 0 & 0 & 0 & 0 \\ 0 & 0 & 0 & 0 & -5 & U & 0 & 0 \\ 0 & 0 & 0 & 0 & U & -5 & 0 & 0 \\ 0 & 0 & 0 & 0 & 0 & 0 & -7 & T \\ 0 & 0 & 0 & 0 & 0 & 0 & T & -3 \end{bmatrix}, \quad (34)$$

where

$$T = -4\sqrt{3}\gamma(\mathbf{q}), \quad U = -8\gamma(\mathbf{q}),$$
$$X = \sqrt{3}\gamma(\mathbf{q}), \quad Y = 2\gamma(\mathbf{q}). \quad (35)$$

Thus, we have the mode energies, with their degeneracies in parentheses:

$$\begin{aligned} \omega_1 &= 3J/2 + 10k/9 - j/18 \ (2), \\ \omega_{2,3} &= 3J/2 + 2k/9 - 5j/18 \pm (4j-2k)\gamma(\mathbf{q})/9, \ (1) \\ \omega_{4,5} &= 3J/2 + 2k/9 - 5j/18 \\ &\quad \pm \sqrt{(4k+j)^2 + 3(k-2j)^2\gamma(\mathbf{q})^2}/9 \ (2). \end{aligned} \quad (36)$$

We determine the polarization of the modes as follows. The mode ω_1 involves state $3A$ which has $\mathcal{S}_{A,z} = -\frac{3}{2}$ or state $6B$ which has $\mathcal{S}_{B,z} = \frac{3}{2}$ and is therefore not accessible via a single spin operator from the $\mathcal{S}_{A,z} = \frac{1}{2}, \mathcal{S}_{B,z} = -\frac{1}{2}$ ground state. The modes ω_2 and ω_3 arise from states $5A$ and $4B$. State $5A$ has $\mathcal{S}_{A,z} = \frac{1}{2}$, which is activated from the $\mathcal{S}_{A,z} = \frac{1}{2}$ ground state by an $\mathcal{S}_{A,z}$ operator and state $4B$ has $\mathcal{S}_{B,z} = -\frac{1}{2}$ which is activated from the $\mathcal{S}_{B,z} = -\frac{1}{2}$ ground state by an $\mathcal{S}_{B,z}$ operator. The modes ω_4 and ω_5 arise from states $4A$, $3B$, $6A$, or $5B$. State $4A$ has $\mathcal{S}_{A,z} = -\frac{1}{2}$, which is activated by an $\mathcal{S}_{A,-}$ operator and state $5B$ has $\mathcal{S}_{B,z} = \frac{1}{2}$ which is activated by an $\mathcal{S}_{B,+}$ operator.

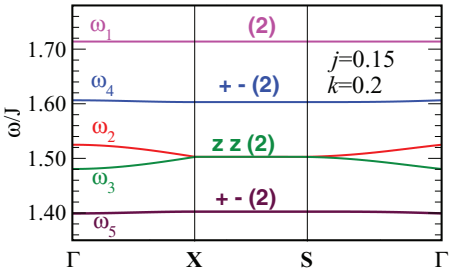

FIG. 6. (Color online) As Fig. 5, but for modes near energy $3J/2$ for the antiferromagnetic configuration. The highest-energy mode is not accessible in linear (in $\mathbf{S}$) response theory.

States $3B$ or $6A$ lead to similar results. These modes (with their polarizations) are shown in Fig. 6.

D. Manifold at energy $3J/2$ for ferromagnetic configuration

The result of the calculation of $V(3J/2)$ for the ferromagnetic configuration is given in Eq. (D44) of Appendix D, which implies, in the notation of Eq. (23), that

$$\mathbf{A}_k = \frac{1}{9}\begin{bmatrix} -10 & 0 & 0 & 0 & 0 & 0 & 0 & 0 \\ 0 & -6 & 0 & 0 & 0 & 1 & 0 & 0 \\ 0 & 0 & -2 & 0 & 0 & 0 & 2 & 0 \\ 0 & 0 & 0 & 2 & 0 & 0 & 0 & 3 \\ 0 & 0 & 0 & 0 & -10 & 0 & 0 & 0 \\ 0 & 1 & 0 & 0 & 0 & -6 & 0 & 0 \\ 0 & 0 & 2 & 0 & 0 & 0 & -2 & 0 \\ 0 & 0 & 0 & 3 & 0 & 0 & 0 & 2 \end{bmatrix}, \quad (37)$$

$$\mathbf{A}_j = \frac{1}{18}\begin{bmatrix} 1 & 0 & 0 & 0 & 0 & 0 & 0 & 0 \\ 0 & 3 & 0 & 0 & 0 & 4 & 0 & 0 \\ 0 & 0 & 5 & 0 & 0 & 0 & 8 & 0 \\ 0 & 0 & 0 & 7 & 0 & 0 & 0 & 12 \\ 0 & 0 & 0 & 0 & 1 & 0 & 0 & 0 \\ 0 & 4 & 0 & 0 & 0 & 3 & 0 & 0 \\ 0 & 0 & 8 & 0 & 0 & 0 & 5 & 0 \\ 0 & 0 & 0 & 12 & 0 & 0 & 0 & 7 \end{bmatrix}, \quad (38)$$

where the rows and column are labeled in the order $3A$, $4A$, $5A$, $6A$, $3B$, $4B$, $5B$, $6B$. We thereby find the mode energies to be

$$\begin{aligned} \omega_{1,2} &= 1.5J + \frac{j-20k}{18}, \\ \omega_{3,4} &= 1.5J + \frac{3j-12k}{18} \pm \frac{k-2j}{9}\gamma(\mathbf{q}), \\ \omega_{5,6} &= 1.5J + \frac{5j-4k}{18} \pm \frac{2k-4j}{9}\gamma(\mathbf{q}), \\ \omega_{7,8} &= 1.5J + \frac{7j+4k}{18} \pm \frac{k-2j}{3}\gamma(\mathbf{q}). \end{aligned} \quad (39)$$

The determination of the polarization of the mode is done as we did for the modes of Eq. (36). The results are shown in Fig. 7.

V. NÉEL SPIN WAVES

In this section, we compare the results obtained above with those from ordinary spin-wave theory. In Fig. 8, we

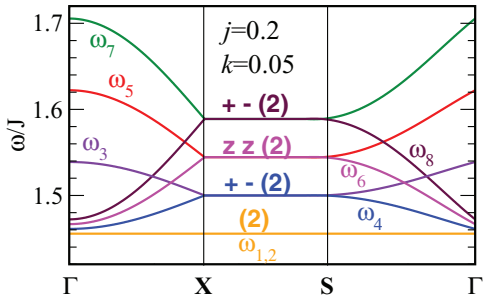

FIG. 7. (Color online) As Fig. 5, but for excitations in the manifold near energy $1.5J$ for the ferromagnetic configuration from Eq. (39). The lowest-energy mode is not accessible in linear (in **S**) response theory.

show the six branches of transverse excitations from the Néel ground state. Note that apart from the lowest manifold, the two approaches lead to quite different spectra. As we showed above, the lowest manifold of trimer excitations is obtained by an exact mapping onto a Néel spin spectrum. One sees that for the antiferromagnetic configuration the energy scale of the lowest branch of spin waves is significantly larger for the trimer approach than for the Néel approach. This is because the trimer approach takes better account of quantum zero-point motion than does the Néel approach. It is well known that zero-point fluctuations tend to increase the spin-wave energies. This is shown by exact calaculations for one-dimensional spin chains[26] and by perturbative calculations for three-dimensional systems.[27] In contrast, for the ferromagnetic configuration, the opposite effect occurs because the energies are proportional to the spin magnitudes.

VI. NEUTRON DIFFRACTION

Some aspects of neutron diffraction have been discussed by Furrer *et al.*[6] and by Qiu *et al.*[7] Here, we discuss briefly the difference between the diffraction spectrum of the trimer system and that of the associated Néel state. The elastic magnetic scattering intensity at wave vector **Q** is

$$\frac{d\sigma}{d\Omega} \approx \sum_{\mathbf{G}} [|\mathbf{F}(\mathbf{Q})|^2 - |\hat{\mathbf{Q}} \cdot \mathbf{F}(\mathbf{Q})|^2] \delta(\mathbf{Q} - \mathbf{G}), \tag{40}$$

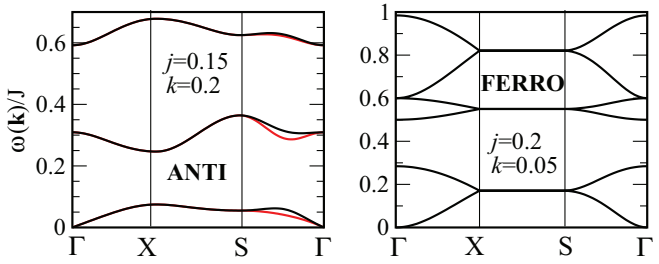

FIG. 8. (Color online) As Fig. 4. Néel (transverse) spin-wave spectrum for the antiferromagnetic (left) and ferromagnetic (right) configurations. Note that the twofold degeneracy of the antiferromagnetic spectrum is broken along the low-symmetry **S**-Γ line.

TABLE II. Structure parameters (Ref. 13) (very similar results are given in Ref. 28) for the distorted kagome system $Cu_2(OD)_3Cl$ (Refs. 11 and 12). Here, x, y, and z are the $P2_1c$ fractional coordinates with respect to axes $\mathbf{a} = 9.1056$ Å, $\mathbf{b} = 6.8151$ Å, and $\mathbf{c} = 11.829$ Å, with $\beta = 30.825^\circ$. We choose the $P2_1c$ setting because the kagome plane is $x \approx 0$ in the this setting. The last column S shows the nonzero spin component in the trimer phase and is taken as along the a, b, and c axes, respectively, in Fig. 9. For the Néel model, we set the spin magnitude to 0.5 instead of $\frac{1}{3}$ and $\frac{1}{6}$. The Cu_3 sites are in the triangular lattice planes which interleave the kagome planes, but our calculations do not include their moments.

Cu sites	x	y	z	S
$Cu_1(1)$	0	0	0	−1/6
$Cu_1(2)$	0	1/2	1/2	1/6
$Cu_2(2)$	0.0072	0.2658	0.2409	−1/3
$Cu_2(3)$	0.9929	0.7658	0.2591	−1/3
$Cu_2(4)$	0.9929	0.7342	0.7591	−1/3
$Cu_2(2)$	0.0072	0.2342	0.7409	1/3
$Cu_3(1)$	1/2	0	1/2	0
$Cu_3(2)$	1/2	1/2	0	0

where **G** is summed over all reciprocal lattice vectors and the magnetic vector structure factor **F** is

$$\mathbf{F}(\mathbf{Q}) \approx \sum_{\tau} \langle \mathbf{S}_\tau \rangle e^{i\mathbf{Q}\cdot\tau}, \tag{41}$$

where τ are the copper spin positions given in Table II and $\langle \mathbf{S}_\tau \rangle$ is the thermal average of the spin at site τ. For the Néel model, we take the spin values as 0.5, while for the trimer model it is $\frac{1}{6}$ and $\frac{1}{3}$ as shown in Table II. To simplify the presentation, we do not discuss the atomic form factor and the Debye-Waller factor. The magnetic elastic diffraction intensities (apart from the thermal and magnetic form factors) are summarized in Fig. 9 for different collinear spin configurations along the crystal axes for both the trimer and Néel models, including AF and F spin configurations. As expected, there are significant differences between the antiferromagnetic and ferromagnetic ordered trimer configurations. Also, for a given spin configuration, the trimer model is significantly different than the Néel model. Due to smaller spin values in the trimer phase, the intensities are much weaker. Hence, observation of the magnetic Bragg peaks would be much more difficult in the trimer phase than for the Néel model. Other than this difference, there are other differences at various scattering angle and it may be possible to distinguish the Néel and trimer model experimentally. In Fig. 9, we also show nuclear scattering, which has some overlap with the strongest magnetic peaks. The unique magnetic peaks are at low angle and there are only a few of them.

VII. INELASTIC SCATTERING CROSS SECTION

In this section, we evaluate the inelastic cross section for the antiferromagnetic configuration at zero temperature. To do this, we will construct the appropriate response functions,

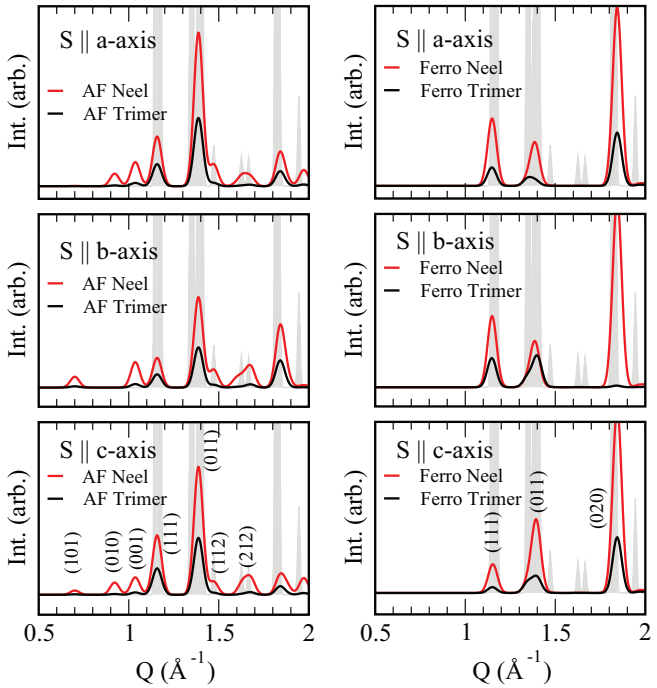

FIG. 9. (Color online) Elastic magnetic Bragg peaks for different spin alignments for trimer and Néel models for the AF (left) and F (right) configurations, respectively. The gray lines in the background show the nuclear scattering.

namely,

$$\langle\langle A;B\rangle\rangle \equiv \sum_n \langle 0|A|n\rangle\langle n|B|0\rangle \delta(E_n - \hbar\omega), \tag{42}$$

where $|0\rangle$ denotes the ground state and the sum is over all states $|n\rangle$ with energy E_n relative to the ground state. Here, the operators A and B are proportional to the Fourier transforms of the spin operators. In particular, we will need

$$\mathcal{S}_{\alpha\beta}(\mathbf{q},\omega) = \langle\langle S_\alpha(\mathbf{q}); S_\beta(-\mathbf{q})\rangle\rangle. \tag{43}$$

Thus,

$$\begin{aligned}
\mathcal{S}_{+-}(\mathbf{q},\omega) &= \sum_n |\langle n|S_-(\mathbf{q})|0\rangle|^2 \delta(E_n - \hbar\omega),\\
\mathcal{S}_{-+}(\mathbf{q},\omega) &= \sum_n |\langle n|S_+(\mathbf{q})|0\rangle|^2 \delta(E_n - \hbar\omega),\\
\mathcal{S}_{zz}(\mathbf{q},\omega) &= \sum_n |\langle n|S_z(\mathbf{q})|0\rangle|^2 \delta(E_n - \hbar\omega).
\end{aligned} \tag{44}$$

(We later set $\hbar = 1$.) To analyze the single-magnon contributions to these quantities we need to relate the spin operators to the normal mode operators. Note that when we evaluate Eq. (44) at zero temperature, only contributions to the operator $S_\beta(\mathbf{q})$ proportional to creation operators are nonzero. We will quote results for the transverse and longitudinal cross sections, given respectively by

$$\begin{aligned}
I_{\text{trans}}(\mathbf{q},\omega) &= \mathcal{S}_{+-}(\mathbf{q},\omega) + \mathcal{S}_{-+}(\mathbf{q},\omega),\\
I_{\text{long}}(\mathbf{q},\omega) &= \mathcal{S}_{zz}(\mathbf{q},\omega).
\end{aligned} \tag{45}$$

In the calculations which follow, we use the notation introduced in Sec. VI.

1. Ground-state excitations

We first consider inelastic scattering from pseudospin waves. Accordingly, we discuss spin-wave theory for this situation. We express the pseudospin operators in terms of boson creation operators $c_A^\dagger$ and $c_B^\dagger$ for the A (up) and B (down) trimers, respectively, as

$$\sigma_z(A) = 1/2 - c_A^\dagger c_A, \quad \sigma_z(B) = -1/2 + c_A^\dagger c_A, \tag{46}$$

and (with $\sigma_\pm = \sigma_x \pm i\sigma_y$)

$$\sigma_-(A) = c_A^\dagger, \quad \sigma_-(B) = c_B. \tag{47}$$

Then, following the standard spin-wave treatment for such a spin-$\frac{1}{2}$ system we write

$$c_A(\mathbf{q}) = N^{-1/2} \sum_{\mathbf{R}\in\mathbf{A}} e^{-i\mathbf{q}\cdot\mathbf{R}} c_A(\mathbf{R}), \tag{48}$$

and similarly for $c_B(\mathbf{q})$, where $\mathbf{R}$ is summed over all the N positions of A trimers. Then, the boson Hamiltonian $\mathcal{H} \equiv \sum_{\mathbf{q}} \mathcal{H}_{\mathbf{q}}$ at quadratic order is

$$\begin{aligned}
\mathcal{H}_{\mathbf{q}} = 2\mathcal{J}\{&c_A^\dagger(\mathbf{q})c_A(\mathbf{q}) + c_B^\dagger(-\mathbf{q})c_B(-\mathbf{q})\\
&+ \gamma(\mathbf{q})[c_A^\dagger(\mathbf{q})c_B^\dagger(-\mathbf{q}) + c_A(\mathbf{q})c_B(-\mathbf{q})]\}.
\end{aligned} \tag{49}$$

Then, the operators which create normal modes are $\rho^\dagger(\mathbf{q})$ and $\eta^\dagger(\mathbf{q})$, which are determined by

$$c_A^\dagger(\mathbf{q}) = l(\mathbf{q})\rho^\dagger(\mathbf{q}) - m(\mathbf{q})\eta(-\mathbf{q}) \tag{50}$$

and

$$c_B(-\mathbf{q}) = -m(\mathbf{q})\rho^\dagger(\mathbf{q}) + l(\mathbf{q})\eta(-\mathbf{q}), \tag{51}$$

where

$$l(\mathbf{q})^2 = \frac{1+\epsilon(\mathbf{q})}{2\epsilon(\mathbf{q})}, \quad m(\mathbf{q})^2 = \frac{1-\epsilon(\mathbf{q})}{2\epsilon(\mathbf{q})}, \quad l(\mathbf{q})m(\mathbf{q}) = \frac{\gamma(\mathbf{q})}{2\epsilon(\mathbf{q})}, \tag{52}$$

with $\epsilon(\mathbf{q}) = [1-\gamma(\mathbf{q})^2]^{1/2}$. Apart from the constant zero-point energy, one has

$$\mathcal{H} = \sum_{\mathbf{q}} \omega(\mathbf{q})[\rho^\dagger(\mathbf{q})\rho(\mathbf{q}) + \eta^\dagger(\mathbf{q})\eta(\mathbf{q})], \tag{53}$$

where Eq. (8) is $\omega(\mathbf{q}) = 2\mathcal{J}\epsilon(\mathbf{q})$.

Using Eq. (4) we note that the Fourier transform of the spin operators is

$$\begin{aligned}
S_\alpha(\mathbf{q}) = {}& N^{-1/2} \sum_{\mathbf{R}\in A} \sigma_\alpha(\mathbf{R}) e^{-i\mathbf{q}\cdot\mathbf{R}} \tau_A(\mathbf{q})\\
&+ N^{-1/2} \sum_{\mathbf{R}\in B} \sigma_\alpha(\mathbf{R}) e^{-i\mathbf{q}\cdot\mathbf{R}} \tau_B(\mathbf{q}).
\end{aligned} \tag{54}$$

Here, we have introduced the trimer form factors

$$\tau_X(\mathbf{q}) = \tfrac{4}{3}\cos(\mathbf{q}\cdot\hat{n}_X) - \tfrac{1}{3}, \tag{55}$$

where $\hat{n}_X$ incorporates the locations of the sites of trimer X relative to its center of gravity:

$$\hat{n}_A = s(0,1/2,\sqrt{3}/2), \quad \hat{n}_B = s(0,-1/2,\sqrt{3}/2). \tag{56}$$

Within the approximation of a Néel state

$$\tau_X(\mathbf{q}) = 2\cos(\mathbf{q}\cdot\hat{n}_X) - 1. \tag{57}$$

When B in Eq. (42) is proportional to $S_-(\mathbf{q})$ we have (at zero temperature)

$$\begin{aligned} B &= \tau_A(\mathbf{q})c_A^\dagger(\mathbf{q}) + \tau_B(\mathbf{q})c_B(-\mathbf{q}) \\ &\to [l(\mathbf{q})\tau_A(\mathbf{q}) - \tau_B(\mathbf{q})m(\mathbf{q})]\rho^\dagger(\mathbf{q}) + \cdots, \end{aligned} \tag{58}$$

where the dots indicate terms involving $\eta(\mathbf{q})$ which do not contribute at zero temperature. In $I_{\rm trans}$ we also have the contribution when B in Eq. (42) is proportional to $S_+(\mathbf{q})$, in which case

$$B = [l(\mathbf{q})\tau_B(\mathbf{q}) - \tau_A(\mathbf{q})m(\mathbf{q})]\eta^\dagger(-\mathbf{q}) + \cdots. \tag{59}$$

Thus, the contribution to the inelastic transverse cross section is given by

$$\begin{aligned} \mathcal{I}_{\rm trans}(\mathbf{q},\omega) &= \{[l(\mathbf{q})^2 + m(\mathbf{q})^2][\tau_A(\mathbf{q})^2 + \tau_B(\mathbf{q})^2] \\ &\quad - 4l(\mathbf{q})m(\mathbf{q})\tau_A(\mathbf{q})\tau_B(\mathbf{q})\}\delta[\omega - \omega(\mathbf{q})] \\ &= \frac{1}{\epsilon(\mathbf{q})}\{[\tau_A(\mathbf{q})^2 + \tau_B(\mathbf{q})^2] \\ &\quad - 2\gamma(\mathbf{q})\tau_A(\mathbf{q})\tau_B(\mathbf{q})\}\delta[\omega - \omega(\mathbf{q})]. \end{aligned} \tag{60}$$

In the case of a standard two-sublattice antiferromagnet, one has the same result but with $\tau_A(\mathbf{q}) = \tau_B(\mathbf{q}) = 1$. In that case, the inelastic scattering cross section for spin waves alternates in intensity as one goes from one Brillouin zone to the next due to the alternating sign of $\gamma(\mathbf{q})$. Here, the result is more complicated because of the form factor of the unit cell, reflected by the factor $\tau_X(\mathbf{q})$.

2. *Excitons near energy J*

To get the response near energy J for the antiferromagnetic case, we need to construct the nonzero matrix elements required to evaluate Eq. (44). To obtain the cross section near energy J we only consider contributions which involve $a_1^\dagger(\mathbf{R})$ or $a_2^\dagger(\mathbf{R})$. From Eq. (16) and following, we see that the only nonzero contributions of this type are,

$$\begin{aligned} S_-(a,\mathbf{R}) &= a_1^\dagger(\mathbf{R})/\sqrt{3} = -S_-(c,\mathbf{R}), \\ S_z(a,\mathbf{R}) &= a_2^\dagger(\mathbf{R})/\sqrt{12} = -S_z(c,\mathbf{R}), \end{aligned} \tag{61}$$

where $\mathbf{R}$ is an A, or up, trimer and

$$\begin{aligned} S_+(a,\mathbf{R}) &= a_2^\dagger(\mathbf{R})/\sqrt{3} = -S_+(c,\mathbf{R}), \\ S_z(a,\mathbf{R}) &= -a_1^\dagger(\mathbf{R})/\sqrt{12} = -S_z(c,\mathbf{R}), \end{aligned} \tag{62}$$

when $\mathbf{R}$ is a B, or down, trimer. These results lead to

$$\begin{aligned} S_-(\mathbf{q}) &= a_{1A}^\dagger(\mathbf{q})[e^{i\mathbf{q}\cdot\mathbf{n}_A} - e^{-i\mathbf{q}\cdot\mathbf{n}_A}]/\sqrt{3} \\ &= (2i/\sqrt{3})\xi_A(\mathbf{q})a_{1A}^\dagger(\mathbf{q}), \end{aligned} \tag{63}$$

where $\xi_X(\mathbf{q}) = \sin(\mathbf{q}\cdot\mathbf{n}_X)$. Similarly,

$$\begin{aligned} S_+(\mathbf{q}) &= (2i/\sqrt{3}]\xi_B(\mathbf{q})a_{2B}^\dagger(\mathbf{q}), \\ S_z(\mathbf{q}) &= (i/\sqrt{3})[\xi_A(\mathbf{q})a_{2A}^\dagger(\mathbf{q}) - \xi_B(\mathbf{q})a_{1B}^\dagger(\mathbf{q})]. \end{aligned} \tag{64}$$

Then, using Eq. (44), we have

$$\begin{aligned} I_{\rm trans} &= [4\xi_A(\mathbf{q})^2/3]\langle\langle a_{1A}; a_{1A}^\dagger\rangle\rangle \\ &\quad + [4\xi_B(\mathbf{q})^2/3]\langle\langle a_{2B}; a_{2B}^\dagger\rangle\rangle, \end{aligned} \tag{65}$$

where Eq. (27) gives

$$\langle\langle a_{1A}; a_{1A}^\dagger\rangle\rangle = \langle\langle a_{2B}; a_{2B}^\dagger\rangle\rangle = \delta[\omega - \omega_{1A}(\mathbf{q})]. \tag{66}$$

Also, Eq. (26) gives

$$\begin{aligned} a_{1B}^\dagger(\mathbf{q}) &= [\rho_+^\dagger(\mathbf{q}) + \rho_-^\dagger(\mathbf{q})]/\sqrt{2}, \\ a_{2A}^\dagger(\mathbf{q}) &= [\rho_+^\dagger(\mathbf{q}) - \rho_-^\dagger(\mathbf{q})]/\sqrt{2}, \end{aligned} \tag{67}$$

so that

$$\begin{aligned} S_z(\mathbf{q}) &= (i/\sqrt{6})([\xi_A(\mathbf{q}) - \xi_B(\mathbf{q})]\rho_+^\dagger(\mathbf{q}) \\ &\quad -[\xi_A(\mathbf{q}) + \xi_B(\mathbf{q})]\rho_-^\dagger(\mathbf{q})]). \end{aligned} \tag{68}$$

Then, we obtain

$$\begin{aligned} &\langle\langle S_z(\mathbf{q}); S_z(-\mathbf{q})\rangle\rangle \\ &\quad = (1/2)[\xi_A(\mathbf{q}) + \xi_B(\mathbf{q})]^2\langle\langle\rho_+(\mathbf{q}); \rho_+^\dagger(\mathbf{q})\rangle\rangle \\ &\qquad + (1/2)[\xi_A(\mathbf{q}) - \xi_B(\mathbf{q})]^2\langle\langle\rho_-(\mathbf{q}); \rho_-^\dagger(\mathbf{q})\rangle\rangle, \end{aligned} \tag{69}$$

where Eq. (28) gives that

$$\langle\langle\rho_\pm(\mathbf{q}); \rho_\pm^\dagger(\mathbf{q})\rangle\rangle = \delta[\omega - \omega_\pm(\mathbf{q})]. \tag{70}$$

3. *Excitons near energy 3J/2*

Here, we keep only contributions involving creation operators $a_n^\dagger$, with $n > 2$. In this case,

$$\begin{aligned} S_-(a,\mathbf{R}) &= -a_{4A}^\dagger/\sqrt{18} = S_-(c,\mathbf{R}), \\ S_-(b,\mathbf{R}) &= 2a_{4A}^\dagger/\sqrt{18}, \\ S_+(a,\mathbf{R}) &= a_{6A}^\dagger/\sqrt{6} = S_+(c,\mathbf{R}), \\ S_+(b,\mathbf{R}) &= -2a_{6A}^\dagger/\sqrt{6}, \\ S_z(a,\mathbf{R}) &= -a_{5A}^\dagger/\sqrt{18} = S_-(c,\mathbf{R}), \\ S_z(b,\mathbf{R}) &= 2a_{5A}^\dagger/\sqrt{18} \end{aligned} \tag{71}$$

when $\mathbf{R}$ is an A, up, site. Also,

$$\begin{aligned} S_+(a,\mathbf{R}) &= a_{5B}^\dagger/\sqrt{18} = S_-(c,\mathbf{R}), \\ S_+(b,\mathbf{R}) &= -2a_{5B}^\dagger/\sqrt{18}, \\ S_-(a,\mathbf{R}) &= -a_{3B}^\dagger/\sqrt{6} = S_-(c,\mathbf{R}), \\ S_-(b,\mathbf{R}) &= 2a_{3B}^\dagger/\sqrt{6}, \\ S_z(a,\mathbf{R}) &= -a_{4B}^\dagger/\sqrt{18} = S_-(c,\mathbf{R}), \\ S_z(b,\mathbf{R}) &= 2a_{4B}^\dagger/\sqrt{18} \end{aligned} \tag{72}$$

when $\mathbf{R}$ is a B, down, site. Thus,

$$\begin{aligned} S_-(\mathbf{q}) &= -\mu_A(\mathbf{q})a_{4A}^\dagger(\mathbf{q})/\sqrt{18} - \mu_B(\mathbf{q})a_{3B}^\dagger(\mathbf{q})/\sqrt{6}, \\ S_+(\mathbf{q}) &= \mu_A(\mathbf{q})a_{6A}^\dagger(\mathbf{q})/\sqrt{6} - \mu_B(\mathbf{q})a_{5B}^\dagger(\mathbf{q})/\sqrt{18}, \\ S_z(\mathbf{q}) &= -[\mu_A(\mathbf{q})a_{5A}^\dagger(\mathbf{q}) + \mu_B(\mathbf{q})a_{4B}^\dagger(\mathbf{q})]/\sqrt{18}, \end{aligned} \tag{73}$$

where

$$\mu_X(\mathbf{q}) = 2\cos(\mathbf{q}\cdot\mathbf{n}_X) - 1. \tag{74}$$

The intensities can be obtained by inverting the transformation which diagonalizes $V(3J/2)$ whose eigenvalues are given in Eq. (36). Since the algebraic expression for the mode

intensities is too complicated to be enlightening, we confine ourselves to some general remarks. We verify that $S_-(\mathbf{q})$ involves the third and fourth rows and columns of the dynamical matrices of Eqs. (33) and (34). Likewise, $S_+(\mathbf{q})$ involves the seventh and eighth rows and columns of the dynamical matrices of Eqs. (33) and (34). Thus, the transverse response is associated with modes ω_4 and ω_5, in agreement with our previous identification. Similarly, we confirm the identification of ω_2 and ω_3 as belonging to the longitudinal response.

VIII. CONCLUSIONS

We may summarize our results as follows.

(a) The lowest-energy modes of the trimer system shown in Fig. 4 are only slightly different from what one gets (see Fig. 8) using the Néel approximation for the ground state. There is a slight difference in symmetry in that the breaking of degeneracy of Néel spin wave in nonspecial directions does not occur in leading order of perturbation theory within the trimer approximation.

(b) The elastic diffraction pattern shows differences (see Fig. 9) which, in principle, allow one to distinguish between a trimer system and one that is closer to the Néel limit.

(c) The excitation spectra at high energy we have obtained show dramatic differences between the trimer and Néel limits. In the former case, well-defined modes appear in the longitudinal response functions. In general, the trimer limit gives rise to many more elementary excitations and thereby provides a conclusive way to identify a system as being in the trimer limit.

(d) A possible future project would be to develop an interpolation scheme to pass between the qualitatively different Néel and trimer limits.

ACKNOWLEDGMENT

A.B.H. was supported in part by a grant from the department of commerce.

APPENDIX A: ANTIFERROMAGNETIC EXCITATIONS AT ENERGY J

Here, position coordinates are given relative to $\mathbf{R}$ a lattice site occupied by an "up" trimer. Thus, $a_2(0)$ denotes $a_2(\mathbf{R})$, $a_1(\boldsymbol{\delta}_1)$ denotes $a_1(\mathbf{R}+\boldsymbol{\delta}_1)$, and so forth. We treat the interaction of one of the spins (a, b, or c) of the trimer at $\mathbf{R}$ with one of the spins (a, b, or c) of a neighboring trimer at $\mathbf{R}+\boldsymbol{\delta}_n$, for $n = 1,2,3,4$. In this section, we drop all terms referring to states $n > 2$ since such states occur at energy $3J/2$. Also, as mentioned, we drop all terms which are off diagonal in J.

1. a at 0 interacts with b at $\boldsymbol{\delta}_3$

Within the band at energy J we may write

$$S_-(a) = a_1^\dagger(0)/\sqrt{3}, \quad S_+(a) = a_1(0)/\sqrt{3}, \tag{A1}$$

$$S_z(a) = \frac{1}{3} + \frac{a_2^\dagger(0)}{\sqrt{12}} + \frac{a_2(0)}{\sqrt{12}} - \frac{n_1(0)}{3} - \frac{n_2(0)}{3} \tag{A2}$$

and

$$S_-(b,\boldsymbol{\delta}_3) = 0, \quad S_+(b,\boldsymbol{\delta}_3) = 0, \tag{A3}$$

$$S_z(b,\boldsymbol{\delta}_3) = \frac{1}{6} - \frac{2n_1(\boldsymbol{\delta}_3)}{3} + \frac{n_2(\boldsymbol{\delta}_3)}{3}. \tag{A4}$$

Thus, this interaction leads to the Hamiltonian

$$\mathcal{H} = j[-2n_1(\boldsymbol{\delta}_3) + n_2(\boldsymbol{\delta}_3)]/9 - j[n_1(0) + n_2(0)]/18. \tag{A5}$$

2. a at 0 interacts with c at $\boldsymbol{\delta}_3$ and $\boldsymbol{\delta}_4$

Here,

$$S_-(a) = a_1^\dagger(0)/\sqrt{3}, \quad S_+(a) = a_1(0)/\sqrt{3}, \tag{A6}$$

$$S_z(a) = \frac{1}{3} + \frac{a_2^\dagger(0)}{\sqrt{12}} + \frac{a_2(0)}{\sqrt{12}} - \frac{n_1(0)}{3} - \frac{n_2(0)}{3}, \tag{A7}$$

and, where δ assumes the values $\boldsymbol{\delta}_3$ and $\boldsymbol{\delta}_4$,

$$S_-(c,\boldsymbol{\delta}) = -a_2(\boldsymbol{\delta})/\sqrt{3}, \tag{A8}$$

$$S_+(c,\boldsymbol{\delta}) = -a_2^\dagger(\boldsymbol{\delta})/\sqrt{3}, \tag{A9}$$

$$S_z(c,\boldsymbol{\delta}) = -1/3 + a_1^\dagger(\boldsymbol{\delta})/\sqrt{12} + a_1(\boldsymbol{\delta})/\sqrt{12} + n_1(\boldsymbol{\delta})/3 + n_2(\boldsymbol{\delta})/3. \tag{A10}$$

Thus, this interaction leads to the Hamiltonian

$$\mathcal{H} = \frac{k}{9}\sum_{\boldsymbol{\delta}}[n_1(\boldsymbol{\delta}) + n_2(\boldsymbol{\delta}) + n_1(0) + n_2(0)] + \frac{k}{12}\sum_{\boldsymbol{\delta}}[a_2^\dagger(0)a_1(\boldsymbol{\delta}) + a_1^\dagger(\boldsymbol{\delta})a_2(0)]. \tag{A11}$$

3. b at 0 interacts with a at $\boldsymbol{\delta}_2$

Here,

$$S_-(b) = 0, \quad S_+(b) = 0, \tag{A12}$$

$$S_z(b) = -1/6 + 2n_2(0)/3 - n_1(0)/3 \tag{A13}$$

and

$$S_-(a,\boldsymbol{\delta}_2) = \frac{a_2(\boldsymbol{\delta}_2)}{\sqrt{3}}, \quad S_+(a,\boldsymbol{\delta}_2) = \frac{a_2^\dagger(\boldsymbol{\delta}_2)}{\sqrt{3}}, \tag{A14}$$

$$S_z(a,\boldsymbol{\delta}_2) = -1/3 - a_1^\dagger(\boldsymbol{\delta}_2)/\sqrt{12} - a_1(\boldsymbol{\delta}_2)/\sqrt{12} + n_1(\boldsymbol{\delta}_2)/3 + n_2(\boldsymbol{\delta}_2)/3. \tag{A15}$$

These interactions lead to the Hamiltonian

$$\mathcal{H} = -j[n_2(\boldsymbol{\delta}_2) + n_1(\boldsymbol{\delta}_2)]/18 + j[n_1(0) - 2n_2(0)]/9. \tag{A16}$$

4. b at 0 interacts with c at $\boldsymbol{\delta}_4$

Here,

$$S_-(b) = 0, \quad S_+(b) = 0, \tag{A17}$$

$$S_z(b) = -1/6 + 2n_2(0)/3 - n_1(0)/3 \tag{A18}$$

and

$$S_-(c,\boldsymbol{\delta}_4) = -\frac{a_2(\boldsymbol{\delta}_4)}{\sqrt{3}}, \quad S_+(c,\boldsymbol{\delta}_4) = -\frac{a_2^\dagger(\boldsymbol{\delta}_4)}{\sqrt{3}}, \tag{A19}$$

$$S_z(c,\boldsymbol{\delta}_4) = -1/3 + a_1^\dagger(\boldsymbol{\delta}_4)/\sqrt{12} + a_1(\boldsymbol{\delta}_4)/\sqrt{12} + n_1(\boldsymbol{\delta}_4)/3 + n_2(\boldsymbol{\delta}_4)/3. \tag{A20}$$

These interactions lead to the Hamiltonian

$$\mathcal{H} = -j[n_1(\boldsymbol{\delta}_4) + n_2(\boldsymbol{\delta}_4)]/18 + j[n_1(0) - 2n_2(0)]/9. \tag{A21}$$

5. c at 0 interacts with a at $\boldsymbol{\delta}_1$ and $\boldsymbol{\delta}_2$

Here,

$$S_-(c) = -a_1^\dagger(0)/\sqrt{3}, \quad S_+(c) = -a_1(0)/\sqrt{3}, \tag{A22}$$

$$S_z(c) = \frac{1}{3} - \frac{a_2^\dagger(0)}{\sqrt{12}} - \frac{a_2(0)}{\sqrt{12}} - \frac{n_1(0)}{3} - \frac{n_2(0)}{3}. \tag{A23}$$

and, where $\boldsymbol{\delta}$ assumes the values $\boldsymbol{\delta}_1$ and $\boldsymbol{\delta}_2$,

$$S_-(a,\boldsymbol{\delta}) = 0, \quad S_+(b,\boldsymbol{\delta}) = 0, \tag{A24}$$

$$S_z(a,\boldsymbol{\delta}) = -1/3 - a_1^\dagger(\boldsymbol{\delta})/\sqrt{12} - a_1(\boldsymbol{\delta})/\sqrt{12} + n_1(\boldsymbol{\delta})/3 + n_2(\boldsymbol{\delta})/3. \tag{A25}$$

These interactions lead to the Hamiltonian

$$\mathcal{H} = \frac{k}{9}\sum_{\boldsymbol{\delta}}[n_1(\boldsymbol{\delta}) + n_2(\boldsymbol{\delta}) + n_1(0) + n_2(0)] + \frac{k}{12}\sum_{\boldsymbol{\delta}}[a_2^\dagger(0)a_1(\boldsymbol{\delta}) + a_1^\dagger(\boldsymbol{\delta})a_2(0)]. \tag{A26}$$

6. c at 0 interacts with b at $\boldsymbol{\delta}_1$

Here,

$$S_-(c) = -a_1^\dagger(0)/\sqrt{3}, \quad S_+(c) = -a_1(0)/\sqrt{3}, \tag{A27}$$

$$S_z(c) = \frac{1}{3} - \frac{a_2^\dagger(0)}{\sqrt{12}} - \frac{a_2(0)}{\sqrt{12}} + \frac{n_1(0)}{3} + \frac{n_2(0)}{3} \tag{A28}$$

and

$$S_-(b,\boldsymbol{\delta}_1) = 0, \quad S_+(b,\boldsymbol{\delta}_1) = 0, \quad S_z(b,\boldsymbol{\delta}_1) = \frac{1}{6} - \frac{2n_1(\boldsymbol{\delta}_1)}{3} + \frac{n_2(\boldsymbol{\delta}_1)}{3}. \tag{A29}$$

These lead to the Hamiltonian

$$\mathcal{H} = -j[n_1(0) + n_2(0)]/18 + j[-2n_1(\boldsymbol{\delta}_1) + n_2(\boldsymbol{\delta}_1)]/9. \tag{A30}$$

7. Summary

Summing all the above contributions, we get the Hamiltonian for the band at energy J for the antiferromagnetic configuration

$$V(J) = \sum_{\mathbf{R}}\Bigg(j[n_1(\mathbf{R}) - 5n_2(\mathbf{R}) + n_2(\mathbf{R}_1) - 5n_1(\mathbf{R}_1)]/9 + 4k[n_1(\mathbf{R}) + n_2(\mathbf{R}) + n_1(\mathbf{R}_1) + n_2(\mathbf{R}_1)]/9 + \sum_{\delta}k[a_2^\dagger(\mathbf{R})a_1(\mathbf{R}+\boldsymbol{\delta}) + a_1^\dagger(\mathbf{R}+\boldsymbol{\delta})a_2(\mathbf{R})]/12\Bigg), \tag{A31}$$

where $\boldsymbol{\delta}$ is summed over the four values shown in Fig. 1.

APPENDIX B: ANTIFERROMAGNETIC EXCITATIONS AT ENERGY $3J/2$

1. a at 0 interacts with b at $\boldsymbol{\delta}_3$

Here,

$$S_-(a) = -a_4^\dagger(0)/\sqrt{18} + a_6(0)/\sqrt{6}, \quad S_+(a) = -a_4(0)/\sqrt{18} + a_6^\dagger(0)/\sqrt{6}, \tag{B1}$$

$$S_z(a) = \frac{1}{3} - \frac{a_5^\dagger(0)}{\sqrt{18}} - \frac{a_5(0)}{\sqrt{18}} + \frac{n_6(0)}{6} - \frac{n_5(0)}{6} - \frac{n_4(0)}{2} - \frac{5n_3(0)}{6} \tag{B2}$$

and

$$S_-(b,\boldsymbol{\delta}_3) = -2a_5(\boldsymbol{\delta}_3)/\sqrt{18} + 2a_3^\dagger(\boldsymbol{\delta}_3)/\sqrt{6}, \tag{B3}$$

$$S_+(b,\boldsymbol{\delta}_3) = -2a_5^\dagger(\boldsymbol{\delta}_3)/\sqrt{18} + 2a_3(\boldsymbol{\delta}_3)/\sqrt{6}, \tag{B4}$$

$$S_z(b,\boldsymbol{\delta}_3) = \frac{1}{6} + \frac{2a_4^\dagger(\boldsymbol{\delta}_3)}{\sqrt{18}} + \frac{2a_4(\boldsymbol{\delta}_3)}{\sqrt{18}} + \frac{n_6(\boldsymbol{\delta}_3)}{3} - \frac{n_4(\boldsymbol{\delta}_3)}{3} - \frac{2n_3(\boldsymbol{\delta}_3)}{3}. \tag{B5}$$

These interactions give rise to the Hamiltonian

$$\mathcal{H} = \sqrt{3}j[-a_4^\dagger(0)a_3(\boldsymbol{\delta}_3) - a_5^\dagger(\boldsymbol{\delta}_3)a_6(0) - a_3^\dagger(\boldsymbol{\delta}_3)a_4(0) - a_6^\dagger(0)a_5(\boldsymbol{\delta}_3)]/18 + j[4n_6(\boldsymbol{\delta}_3) - 4n_4(\boldsymbol{\delta}_3) - 8n_3(\boldsymbol{\delta}_3) + n_6(0) - n_5(0) - 3n_4(0) - 5n_3(0)]/36 + j[-a_5^\dagger(0)a_4(\boldsymbol{\delta}_3) - a_5(0)a_4^\dagger(\boldsymbol{\delta}_3)]/9. \tag{B6}$$

2. a at 0 interacts with c at $\boldsymbol{\delta}_3$ and $\boldsymbol{\delta}_4$

Here,

$$S_-(a) = -a_4^\dagger(0)/\sqrt{18} + a_6(0)/\sqrt{6}, \tag{B7}$$

$$S_+(a) = -a_4(0)/\sqrt{18} + a_6^\dagger(0)/\sqrt{6}, \tag{B8}$$

$$S_z(a) = \frac{1}{3} - \frac{a_5^\dagger(0)}{\sqrt{18}} - \frac{a_5(0)}{\sqrt{18}} + \frac{n_6(0)}{6} - \frac{n_5(0)}{6} - \frac{n_4(0)}{2} - \frac{5n_3(0)}{6}, \tag{B9}$$

and, with $\boldsymbol{\delta} = \boldsymbol{\delta}_3$ or $\boldsymbol{\delta} = \boldsymbol{\delta}_4$, we have

$$S_-(c,\boldsymbol{\delta}) = a_5(\boldsymbol{\delta})/\sqrt{18} - a_3^\dagger(\boldsymbol{\delta})/\sqrt{6}, \tag{B10}$$

$$S_+(c,\boldsymbol{\delta}) = a_5^\dagger(\boldsymbol{\delta})/\sqrt{18} - a_3(\boldsymbol{\delta})/\sqrt{6}, \tag{B11}$$

$$S_z(c,\boldsymbol{\delta}) = -\frac{1}{3} - \frac{a_4^\dagger(\boldsymbol{\delta})}{\sqrt{18}} - \frac{a_4(\boldsymbol{\delta})}{\sqrt{18}} + \frac{5n_6(\boldsymbol{\delta})}{6} + \frac{n_5(\boldsymbol{\delta})}{2} + \frac{n_4(\boldsymbol{\delta})}{6} - \frac{n_3(\boldsymbol{\delta})}{6}. \tag{B12}$$

These interactions lead to the Hamiltonian

$$\mathcal{H} = \sum_{\boldsymbol{\delta}} \Big(\frac{\sqrt{3}k}{36}[a_4^\dagger(0)a_3(\boldsymbol{\delta}) + a_5^\dagger(\boldsymbol{\delta})a_6(0) + a_6^\dagger(0)a_5(\boldsymbol{\delta}) + a_3^\dagger(\boldsymbol{\delta})a_4(0)] + \frac{k}{18}[5n_6(\boldsymbol{\delta}) + 3n_5(\boldsymbol{\delta}) + n_4(\boldsymbol{\delta}) - n_3(\boldsymbol{\delta}) - n_6(0) + n_5(0) + 3n_4(0) + 5n_3(0)] + \frac{k}{18}[a_5^\dagger(0)a_4(\boldsymbol{\delta}) + a_4^\dagger(\boldsymbol{\delta})a_5(0)]\Big). \tag{B13}$$

3. b at 0 interacts with a at $\boldsymbol{\delta}_2$

Here,

$$S_-(b) = 2a_4^\dagger(0)/\sqrt{18} - 2a_6(0)/\sqrt{6}, \tag{B14}$$

$$S_+(b) = 2a_4(0)/\sqrt{18} - 2a_6^\dagger(0)/\sqrt{6}, \tag{B15}$$

$$S_z(b) = -\frac{1}{6} + \frac{2a_5^\dagger(0)}{\sqrt{18}} + \frac{2a_5(0)}{\sqrt{18}} + \frac{2n_6(0)}{3} + \frac{n_5(0)}{3} - \frac{n_3(0)}{3} \tag{B16}$$

and

$$S_-(a,\boldsymbol{\delta}_2) = a_5(\boldsymbol{\delta}_2)/\sqrt{18} - a_3^\dagger(\boldsymbol{\delta}_2)/\sqrt{6}, \quad S_+(a,\boldsymbol{\delta}_2) = a_5^\dagger(\boldsymbol{\delta}_2)/\sqrt{18} - a_3(\boldsymbol{\delta}_2)/\sqrt{6}, \tag{B17}$$

$$S_z(a,\boldsymbol{\delta}_2) = -\frac{1}{3} - \frac{a_4^\dagger(\boldsymbol{\delta}_2)}{\sqrt{18}} - \frac{a_4(\boldsymbol{\delta}_2)}{\sqrt{18}} + \frac{5n_6(\boldsymbol{\delta}_2)}{6} + \frac{n_5(\boldsymbol{\delta}_2)}{2} + \frac{n_4(\boldsymbol{\delta}_2)}{6} - \frac{n_3(\boldsymbol{\delta}_2)}{6}. \tag{B18}$$

Thus, the Hamiltonian for this interaction is

$$\mathcal{H} = \sqrt{3}j[-a_4^\dagger(0)a_3(\boldsymbol{\delta}_2) - a_5^\dagger(\boldsymbol{\delta}_2)a_6(0) - a_3^\dagger(\boldsymbol{\delta}_2)a_4(0) - a_6^\dagger(0)a_5(\boldsymbol{\delta}_2)]/18 + j[-5n_6(\boldsymbol{\delta}_2) - 3n_5(\boldsymbol{\delta}_2) - n_4(\boldsymbol{\delta}_2) + n_3(\boldsymbol{\delta}_2) - 8n_6(0) - 4n_5(0) + 4n_3(0)]/36 + j[-a_5^\dagger(0)a_4(\boldsymbol{\delta}_2) - a_4^\dagger(\boldsymbol{\delta}_2)a_5(0)]/9. \tag{B19}$$

4. b at 0 interacts with c at $\boldsymbol{\delta}_4$

Here,

$$S_-(b) = 2a_4^\dagger(0)/\sqrt{18} - 2a_6(0)/\sqrt{6}, \tag{B20}$$

$$S_+(b) = 2a_4(0)/\sqrt{18} - 2a_6^\dagger(0)/\sqrt{6}, \tag{B21}$$

$$S_z(b) = -\frac{1}{6} + \frac{2a_5^\dagger(0)}{\sqrt{18}} + \frac{2a_5(0)}{\sqrt{18}} + \frac{2n_6(0)}{3} + \frac{n_5(0)}{3} - \frac{n_3(0)}{3} \tag{B22}$$

and

$$S_-(c,\boldsymbol{\delta}_4) = a_5(\boldsymbol{\delta}_4)/\sqrt{18} - a_3^\dagger(\boldsymbol{\delta}_4)/\sqrt{6}, \quad S_+(c,\boldsymbol{\delta}_4) = a_5^\dagger(\boldsymbol{\delta}_4)/\sqrt{18} - a_3(\boldsymbol{\delta}_4)/\sqrt{6},$$

$$S_z(c,\boldsymbol{\delta}_4) = -\frac{1}{3} - \frac{a_4^\dagger(\boldsymbol{\delta}_4)}{\sqrt{18}} - \frac{a_4(\boldsymbol{\delta}_4)}{\sqrt{18}} + \frac{5n_6(\boldsymbol{\delta}_4)}{6} + \frac{n_5(\boldsymbol{\delta}_4)}{2} + \frac{n_4(\boldsymbol{\delta}_4)}{6} - \frac{n_3(\boldsymbol{\delta}_4)}{6}. \tag{B23}$$

These results lead to the Hamiltonian

$$\mathcal{H} = \sqrt{3}j[-a_4^\dagger(0)a_3(\boldsymbol{\delta}_4) - a_5^\dagger(\boldsymbol{\delta}_4)a_6(0) - a_3^\dagger(\boldsymbol{\delta}_4)a_4(0) - a_6^\dagger(0)a_5(\boldsymbol{\delta}_4)]/18 + j[-5n_6(\boldsymbol{\delta}_4) - 3n_5(\boldsymbol{\delta}_4) - n_4(\boldsymbol{\delta}_4) + n_3(\boldsymbol{\delta}_4) - 8n_6(0) - 4n_5(0) + 4n_3(0)]/36 + j[-a_5^\dagger(0)a_4(\boldsymbol{\delta}_4) - a_4^\dagger(\boldsymbol{\delta}_4)a_5(0)]/9. \tag{B24}$$

5. c at 0 interacts with a at $\boldsymbol{\delta}_1$ and $\boldsymbol{\delta}_2$

Here,

$$S_-(c) = -a_4^\dagger(0)/\sqrt{18} + a_6(0)/\sqrt{6}, \tag{B25}$$

$$S_+(c) = -a_4(0)/\sqrt{18} + a_6^\dagger(0)/\sqrt{6}, \tag{B26}$$

$$S_z(c) = \frac{1}{3} - \frac{a_5^\dagger(0)}{\sqrt{18}} - \frac{a_5(0)}{\sqrt{18}} + \frac{n_6(0)}{6} - \frac{n_5(0)}{6} - \frac{n_4(0)}{2} - \frac{5n_3(0)}{6} \tag{B27}$$

and, where $\boldsymbol{\delta}$ assumes the values $\boldsymbol{\delta}_1$ and $\boldsymbol{\delta}_2$,

$$S_-(a,\boldsymbol{\delta}) = a_5(\boldsymbol{\delta})/\sqrt{18} - a_3^\dagger(\boldsymbol{\delta})/\sqrt{6}, \quad S_+(a,\boldsymbol{\delta}) = a_5^\dagger(\boldsymbol{\delta})/\sqrt{18} - a_3(\boldsymbol{\delta})/\sqrt{6}, \tag{B28}$$

$$S_z(a,\boldsymbol{\delta}) = -\frac{1}{3} - \frac{a_4^\dagger(\boldsymbol{\delta})}{\sqrt{18}} - \frac{a_4(\boldsymbol{\delta})}{\sqrt{18}} + \frac{5n_6(\boldsymbol{\delta})}{6} + \frac{n_5(\boldsymbol{\delta})}{2} + \frac{n_4(\boldsymbol{\delta})}{6} - \frac{n_3(\boldsymbol{\delta})}{6}. \tag{B29}$$

Thus, the Hamiltonian from this interaction is

$$\mathcal{H} = \sum_{\boldsymbol{\delta}} \Big(\frac{\sqrt{3}k}{36}[a_4^\dagger(0)a_3(\boldsymbol{\delta}) + a_6(0)a_5^\dagger(\boldsymbol{\delta}) + a_4(0)a_3^\dagger(\boldsymbol{\delta}) + a_6^\dagger(0)a_5(\boldsymbol{\delta})] + \frac{k}{18}[5n_6(\boldsymbol{\delta}) + 3n_5(\boldsymbol{\delta}) + n_4(\boldsymbol{\delta}) - n_3(\boldsymbol{\delta}) - 2n_6(0) + 2n_5(0) + 6n_4(0) + 10n_3(0) + a_5^\dagger(0)a_4(\boldsymbol{\delta}) + a_5(0)a_4^\dagger(\boldsymbol{\delta})]\Big). \tag{B30}$$

6. c at 0 interacts with b at $\boldsymbol{\delta}_1$

Here,

$$S_-(c) = -a_4^\dagger(0)/\sqrt{18} + a_6(0)/\sqrt{6}, \tag{B31}$$

$$S_+(c) = -a_4(0)/\sqrt{18} + a_6^\dagger(0)/\sqrt{6}, \tag{B32}$$

$$S_z(c) = \frac{1}{3} - \frac{a_5^\dagger(0)}{\sqrt{18}} - \frac{a_5(0)}{\sqrt{18}} + \frac{n_6(0)}{6} - \frac{n_5(0)}{6} - \frac{n_4(0)}{2} - \frac{5n_3(0)}{6} \tag{B33}$$

and

$$S_-(b,\boldsymbol{\delta}_1) = -2a_5(\boldsymbol{\delta}_1)/\sqrt{18} + 2a_3^\dagger(\boldsymbol{\delta}_1)/\sqrt{6}, \quad \text{(B34)}$$

$$S_+(b,\boldsymbol{\delta}_1) = -2a_5^\dagger(\boldsymbol{\delta}_1)/\sqrt{18} + 2a_3(\boldsymbol{\delta}_1)/\sqrt{6}, \quad \text{(B35)}$$

$$S_z(b,\boldsymbol{\delta}_1) = \frac{1}{6} + \frac{2a_4^\dagger(\boldsymbol{\delta}_1)}{\sqrt{18}} + \frac{2a_4(\boldsymbol{\delta}_1)}{\sqrt{18}} + \frac{n_6(\boldsymbol{\delta}_1)}{3} - \frac{n_4(\boldsymbol{\delta}_1)}{3} - \frac{2n_3(\boldsymbol{\delta}_1)}{3}. \quad \text{(B36)}$$

Thus, the Hamiltonian from this interaction is

$$\begin{aligned}\mathcal{H} = {}& \sqrt{3}j[-a_4^\dagger(0)a_3(\boldsymbol{\delta}) - a_5^\dagger(\boldsymbol{\delta})a_6(0) \\ & - a_3^\dagger(\boldsymbol{\delta})a_4(0) - a_6^\dagger(0)a_5(\boldsymbol{\delta})]/18 \\ & + j[4n_6(\boldsymbol{\delta}) - 4n_4(\boldsymbol{\delta}) - 8n_3(\boldsymbol{\delta}) + n_6(0) \\ & - n_5(0) - 3n_4(0) - 5n_3(0)]/36 \\ & + j[-a_5^\dagger(0)a_4(\boldsymbol{\delta}) - a_4^\dagger(\boldsymbol{\delta})a_5(0)]/9. \end{aligned} \quad \text{(B37)}$$

7. Summary

Summing all the above contributions, we get the Hamiltonian for the band at energy $3J/2$ for the antiferromagnetic configuration

$$\begin{aligned} V(3J/2) = {}& j\sum_{\mathbf{R}}\Big[[-n_3(\mathbf{R}) - 3n_4(\mathbf{R}) - 5n_5(\mathbf{R}) - 7n_6(\mathbf{R}) \\ & - n_6(\mathbf{R}_1) - 3n_5(\mathbf{R}_1) - 5n_4(\mathbf{R}_1) - 7n_3(\mathbf{R}_1)]/18 \\ & + \sum_{\boldsymbol{\delta}}(-[a_5^\dagger(\mathbf{R})a_4(\mathbf{R}+\boldsymbol{\delta}) + a_4^\dagger(\mathbf{R}+\boldsymbol{\delta})a_5(\mathbf{R})]/9 \\ & - \sqrt{3}[a_4^\dagger(\mathbf{R})a_3(\mathbf{R}+\boldsymbol{\delta}) + a_3^\dagger(\mathbf{R}+\boldsymbol{\delta})a_4(\mathbf{R}) \\ & + a_5^\dagger(\mathbf{R}+\boldsymbol{\delta})a_6(\mathbf{R}) + a_6^\dagger(\mathbf{R})a_5(\mathbf{R}+\boldsymbol{\delta})]/18)\Big] \\ & + k\sum_{\mathbf{R}}\Big[2[-n_6(\mathbf{R}) + n_5(\mathbf{R}) + 3n_4(\mathbf{R}) + 5n_3(\mathbf{R}) \\ & + 5n_6(\mathbf{R}_1) + 3n_5(\mathbf{R}_1) + n_4(\mathbf{R}_1) - n_3(\mathbf{R}_1)]/9 \\ & + \sum_{\boldsymbol{\delta}}(\sqrt{3}[a_4^\dagger(\mathbf{R})a_3(\mathbf{R}+\boldsymbol{\delta}) + a_3^\dagger(\mathbf{R}+\boldsymbol{\delta})a_4(\mathbf{R}) \\ & + a_5^\dagger(\mathbf{R}+\boldsymbol{\delta})a_6(\mathbf{R}) + a_6^\dagger(\mathbf{R})a_5(\mathbf{R}+\boldsymbol{\delta})]/36 \\ & + [a_5^\dagger(\mathbf{R})a_4(\mathbf{R}+\boldsymbol{\delta}) + a_4^\dagger(\mathbf{R}+\boldsymbol{\delta})a_5(\mathbf{R})]/18)\Big]. \end{aligned} \quad \text{(B38)}$$

APPENDIX C: FERROMAGNETIC EXCITATIONS AT ENERGY J

1. a at 0 interacts with b at $\boldsymbol{\delta}_3$

Here,

$$S_-(a) = a_1^\dagger(0)/\sqrt{3}, \quad S_+(a) = a_1(0)/\sqrt{3}, \quad \text{(C1)}$$

$$S_z(a) = \frac{1}{3} + \frac{a_2^\dagger(0)}{\sqrt{12}} + \frac{a_2(0)}{\sqrt{12}} - \frac{n_1(0)}{3} - \frac{n_2(0)}{3} \quad \text{(C2)}$$

and

$$S_-(b,\boldsymbol{\delta}_3) = 0, \quad S_+(b,\boldsymbol{\delta}_3) = 0, \quad \text{(C3)}$$

$$S_z(b,\boldsymbol{\delta}_3) = -\frac{1}{6} - \frac{n_1(\boldsymbol{\delta}_3)}{3} + \frac{2n_2(\boldsymbol{\delta}_3)}{3}. \quad \text{(C4)}$$

These results lead to the Hamiltonian

$$\mathcal{H} = j[2n_2(\boldsymbol{\delta}_3) - n_1(\boldsymbol{\delta}_3)]/9 + j[n_1(0) + n_2(0)]/18. \quad \text{(C5)}$$

2. a at 0 interacts with c at $\boldsymbol{\delta}_3$ and $\boldsymbol{\delta}_4$

Here,

$$S_-(a) = a_1^\dagger(0)/\sqrt{3}, \quad S_+(a) = a_1(0)/\sqrt{3}, \quad \text{(C6)}$$

$$S_z(a) = \frac{1}{3} + \frac{a_2^\dagger(0)}{\sqrt{12}} + \frac{a_2(0)}{\sqrt{12}} - \frac{n_1(0)}{3} - \frac{n_2(0)}{3} \quad \text{(C7)}$$

and, where $\boldsymbol{\delta}$ assumes the values $\boldsymbol{\delta}_3$ and $\boldsymbol{\delta}_4$,

$$S_-(c,\boldsymbol{\delta}) = -\frac{a_1^\dagger(\boldsymbol{\delta})}{\sqrt{3}}, \quad S_+(c,\boldsymbol{\delta}) = -\frac{a_1(\boldsymbol{\delta})}{\sqrt{3}}, \quad \text{(C8)}$$

$$S_z(c,\boldsymbol{\delta}) = 1/3 - a_2^\dagger(\boldsymbol{\delta})/\sqrt{12} - a_2(\boldsymbol{\delta})/\sqrt{12} - n_1(\boldsymbol{\delta})/3 - n_2(\boldsymbol{\delta})/3. \quad \text{(C9)}$$

Thus, we have that

$$\begin{aligned}\mathcal{H} = \sum_{\boldsymbol{\delta}}\Big(& -\frac{k}{9}[n_1(\boldsymbol{\delta}) + n_2(\boldsymbol{\delta}) + n_1(0) + n_2(0)] \\ & + \frac{k}{12}[-a_2^\dagger(\boldsymbol{\delta})a_2(0) - a_2^\dagger(\boldsymbol{\delta})a_2(0)] \\ & - \frac{k}{6}[a_1^\dagger(0)a_1(\boldsymbol{\delta}) + a_1^\dagger(\boldsymbol{\delta})a_1(0)]\Big). \end{aligned} \quad \text{(C10)}$$

3. b at 0 interacts with a at $\boldsymbol{\delta}_2$

Here,

$$S_-(b) = 0, \quad S_+(b) = 0, \quad \text{(C11)}$$

$$S_z(b) = -\frac{1}{6} + \frac{2n_2(0)}{3} - \frac{n_1(0)}{3} \quad \text{(C12)}$$

and

$$S_-(a,\boldsymbol{\delta}_2) = \frac{a_1^\dagger(\boldsymbol{\delta}_2)}{\sqrt{3}}, \quad S_+(a,\boldsymbol{\delta}_2) = \frac{a_1(\boldsymbol{\delta}_2)}{\sqrt{3}}, \quad \text{(C13)}$$

$$S_z(a,\boldsymbol{\delta}_2) = 1/3 + a_2^\dagger(\boldsymbol{\delta}_2)/\sqrt{12} + a_2(\boldsymbol{\delta}_2)/\sqrt{12} - n_1(\boldsymbol{\delta}_2)/3 - n_2(\boldsymbol{\delta}_2)/3. \quad \text{(C14)}$$

Thus, we obtain the Hamiltonian

$$\mathcal{H} = j[n_1(\boldsymbol{\delta}_2) + n_2(\boldsymbol{\delta}_2)]/18 + j[-n_1(0) + 2n_2(0)]/9. \quad \text{(C15)}$$

4. b at 0 interacts with c at $\boldsymbol{\delta}_4$

Here,

$$S_-(b) = 0, \quad S_+(b) = 0, \quad \text{(C16)}$$

$$S_z(b) = -\frac{1}{6} + \frac{2n_2(0)}{3} - \frac{n_1(0)}{3} \quad \text{(C17)}$$

and

$$S_-(c,\boldsymbol{\delta}_4) = -\frac{a_1^\dagger(\boldsymbol{\delta}_4)}{\sqrt{3}}, \quad S_+(c,\boldsymbol{\delta}_4) = -\frac{a_1(\boldsymbol{\delta}_4)}{\sqrt{3}}, \quad \text{(C18)}$$

$$S_z(c,\boldsymbol{\delta}_4) = 1/3 - a_2^\dagger(\boldsymbol{\delta}_4)/\sqrt{12} - a_2(\boldsymbol{\delta}_4)/\sqrt{12} - n_1(\boldsymbol{\delta}_4)/3 - n_2(\boldsymbol{\delta}_4)/3. \quad \text{(C19)}$$

These interactions give rise to the Hamiltonian

$$\mathcal{H} = j[n_1(\boldsymbol{\delta}_4) + n_2(\boldsymbol{\delta}_4)]/18 + j[-n_1(0) + 2n_2(0)]9. \quad \text{(C20)}$$

5. c at 0 interacts with a at $\boldsymbol{\delta}_1$ and $\boldsymbol{\delta}_2$

Here,

$$S_-(c) = -\frac{a_1^\dagger(0)}{\sqrt{3}}, \quad S_+(c) = -\frac{a_1(0)}{\sqrt{3}}, \quad \text{(C21)}$$

$$S_z(c) = 1/3 - a_2^\dagger(0)/\sqrt{12} - a_2(0)/\sqrt{12} - n_1(0)/3 - n_2(0)/3 \quad \text{(C22)}$$

and, where $\boldsymbol{\delta}$ assumes the values $\boldsymbol{\delta}_1$ and $\boldsymbol{\delta}_2$,

$$S_-(a,\boldsymbol{\delta}) = \frac{a_1^\dagger(\boldsymbol{\delta})}{\sqrt{3}}, \quad S_+(a,\boldsymbol{\delta}) = \frac{a_1(\boldsymbol{\delta})}{\sqrt{3}}, \quad \text{(C23)}$$

$$S_z(a,\boldsymbol{\delta}) = 1/3 + a_2^\dagger(\boldsymbol{\delta})/\sqrt{12} + a_2(\boldsymbol{\delta})/\sqrt{12} - n_1(\boldsymbol{\delta})/3 - n_2(\boldsymbol{\delta})/3. \quad \text{(C24)}$$

These results lead to the Hamiltonian

$$\mathcal{H} = \sum_{\boldsymbol{\delta}}\Bigg[-\frac{k}{9}(n_1(\boldsymbol{\delta}) + n_2(\boldsymbol{\delta}) + n_1(0) + n_2(0)) - \frac{k}{12}(a_2^\dagger(0)a_2(\boldsymbol{\delta}) + a_2^\dagger(\boldsymbol{\delta})a_2(0)) - \frac{k}{6}(a_1^\dagger(0)a_1(\boldsymbol{\delta}) + a_1^\dagger(\boldsymbol{\delta})a_1(0))\Bigg]. \quad \text{(C25)}$$

6. c at 0 interacts with b at $\boldsymbol{\delta}_1$

Here,

$$S_-(c) = -\frac{a_1^\dagger(0)}{\sqrt{3}}, \quad S_+(c) = -\frac{a_1(0)}{\sqrt{3}}, \quad \text{(C26)}$$

$$S_z(c) = \frac{1}{3} - \frac{a_2^\dagger(0)}{\sqrt{12}} - \frac{a_2(0)}{\sqrt{12}} - \frac{n_1(0)}{3} - \frac{n_2(0)}{3} \quad \text{(C27)}$$

and

$$S_-(b,\boldsymbol{\delta}_1) = 0, \quad S_+(b,\boldsymbol{\delta}_1) = 0, \quad \text{(C28)}$$

$$S_z(b,\boldsymbol{\delta}_1) = -\frac{1}{6} + \frac{2n_2(\boldsymbol{\delta}_1)}{3} - \frac{n_1(\boldsymbol{\delta}_1)}{3}. \quad \text{(C29)}$$

These terms give rise to the Hamiltonian

$$\mathcal{H} = j[n_1(0) + n_2(0)]/18 + j[2n_2(\boldsymbol{\delta}_1) - n_1(\boldsymbol{\delta}_1)]/9. \quad \text{(C30)}$$

7. Summary

Summing all the above contributions, we get the Hamiltonian for the band at energy J for the ferromagnetic configuration as

$$V(J) = \sum_{\mathbf{R}}\Bigg[j[5n_2(\mathbf{R}) - n_1(\mathbf{R}) - n_1(\mathbf{R}_1) + 5n_2(\mathbf{R}_1)] - 4k[n_1(\mathbf{R}) + n_2(\mathbf{R}) + n_1(\mathbf{R}_1) + n_2(\mathbf{R}_1)]/9 - \frac{k}{12}\sum_{\boldsymbol{\delta}}([2a_1^\dagger(\mathbf{R})a_1(\mathbf{R}+\boldsymbol{\delta}) + a_2^\dagger(\mathbf{R})a_2(\mathbf{R}+\boldsymbol{\delta}) + 2a_1^\dagger(\mathbf{R}+\boldsymbol{\delta})a_1(\mathbf{R}) + a_2^\dagger(\mathbf{R}+\boldsymbol{\delta})a_2(\mathbf{R})])\Bigg]. \quad \text{(C31)}$$

APPENDIX D: FERROMAGNETIC EXCITATIONS AT ENERGY $3J/2$

1. a at 0 interacts with b at $\boldsymbol{\delta}_3$

Here,

$$S_-(a) = -a_4^\dagger(0)/\sqrt{18} + a_6(0)/\sqrt{6}, \quad \text{(D1)}$$

$$S_+(a) = -a_4(0)/\sqrt{18} + a_6^\dagger(0)/\sqrt{6}, \quad \text{(D2)}$$

$$S_z(a) = \frac{1}{3} - \frac{a_5^\dagger(0)}{\sqrt{18}} - \frac{a_5(0)}{\sqrt{18}} + \frac{n_6(0)}{6} - \frac{n_5(0)}{6} - \frac{n_4(0)}{2} - \frac{5n_3(0)}{6} \quad \text{(D3)}$$

and

$$S_-(b,\boldsymbol{\delta}_3) = 2a_4^\dagger(\boldsymbol{\delta}_3)/\sqrt{18} - 2a_6(\boldsymbol{\delta}_3)/\sqrt{6}, \quad \text{(D4)}$$

$$S_+(b,\boldsymbol{\delta}_3) = 2a_4(\boldsymbol{\delta}_3)/\sqrt{18} - 2a_6^\dagger(\boldsymbol{\delta}_3)/\sqrt{6}, \quad \text{(D5)}$$

$$S_z(b,\boldsymbol{\delta}) = -1/6 + 2a_5^\dagger(\boldsymbol{\delta}_3)/\sqrt{18} + 2a_5(\boldsymbol{\delta}_3)/\sqrt{18} + 2n_6(\boldsymbol{\delta}_3)/3 + n_5(\boldsymbol{\delta}_3)/3 - n_3(\boldsymbol{\delta}_3)/3. \quad \text{(D6)}$$

Thus, these interactions lead to the Hamiltonian

$$\mathcal{H} = j[-a_4^\dagger(0)a_4(\boldsymbol{\delta}_3) - 3a_6^\dagger(\boldsymbol{\delta}_3)a_6(0) - a_4^\dagger(\boldsymbol{\delta}_3)a_4(0) - 3a_6^\dagger(0)a_6(\boldsymbol{\delta}_3)]/18 + j[-4n_3(\boldsymbol{\delta}_3) + 4n_5(\boldsymbol{\delta}_3) + 8n_6(\boldsymbol{\delta}_3) - n_6(0) + n_5(0) + 3n_4(0) + 5n_3(0)]/36 + j[-a_5^\dagger(0)a_5(\boldsymbol{\delta}_3) - a_5^\dagger(\boldsymbol{\delta}_3)a_5(0)]/9. \quad \text{(D7)}$$

2. a at 0 interacts with c at $\boldsymbol{\delta}_3$ and $\boldsymbol{\delta}_4$

Here,

$$S_-(a) = -a_4^\dagger(0)/\sqrt{18} + a_6(0)/\sqrt{6}, \quad \text{(D8)}$$

$$S_+(a) = -a_4(0)/\sqrt{18} + a_6^\dagger(0)/\sqrt{6}, \quad \text{(D9)}$$

$$S_z(a) = \frac{1}{3} - \frac{a_5^\dagger(0)}{\sqrt{18}} - \frac{a_5(0)}{\sqrt{18}} + \frac{n_6(0)}{6} - \frac{n_5(0)}{6} - \frac{n_4(0)}{2} - \frac{5n_3(0)}{6} \quad \text{(D10)}$$

and, where $\boldsymbol{\delta}$ assumes the values $\boldsymbol{\delta}_3$ and $\boldsymbol{\delta}_4$,

$$S_-(c,\boldsymbol{\delta}) = -a_4^\dagger(\boldsymbol{\delta})/\sqrt{18} + a_6(\boldsymbol{\delta})/\sqrt{6}, \quad \text{(D11)}$$

$$S_+(c,\boldsymbol{\delta}) = -a_4(\boldsymbol{\delta})/\sqrt{18} + a_6^\dagger(\boldsymbol{\delta})/\sqrt{6}, \quad \text{(D12)}$$

$$S_z(c,\boldsymbol{\delta}) = \frac{1}{3} - \frac{a_5^\dagger(\boldsymbol{\delta})}{\sqrt{18}} - \frac{a_5(\boldsymbol{\delta})}{\sqrt{18}} - \frac{5n_3(\boldsymbol{\delta})}{6} \quad \text{(D13)}$$

$$- \frac{n_4(\boldsymbol{\delta})}{2} - \frac{n_5(\boldsymbol{\delta})}{6} + \frac{n_6(\boldsymbol{\delta})}{6}. \quad \text{(D14)}$$

Thus,

$$\mathcal{H} = \sum_{\boldsymbol{\delta}} \Big(\frac{k}{36}[a_4^\dagger(\boldsymbol{\delta})a_4(0) + 3a_6^\dagger(\boldsymbol{\delta})a_6(0) + a_4^\dagger(0)a_4(\boldsymbol{\delta}) + 3a_6^\dagger(0)a_6(\boldsymbol{\delta})] + \frac{k}{18}[-5n_3(\boldsymbol{\delta}) - 3n_4(\boldsymbol{\delta}) - n_5(\boldsymbol{\delta}) + n_6(\boldsymbol{\delta}) + n_6(0) - n_5(0) - 3n_4(0) - 5n_3(0)] + \frac{k}{18}[a_5^\dagger(0)a_5(\boldsymbol{\delta}) + a_5^\dagger(\boldsymbol{\delta}_3)a_5(0)] \Big). \tag{D15}$$

3. b at 0 interacts with a at $\boldsymbol{\delta}_2$

$$S_-(b) = 2a_4^\dagger(0)/\sqrt{18} - 2a_6(0)/\sqrt{6}, \tag{D16}$$

$$S_+(b) = 2a_4(0)/\sqrt{18} - 2a_6^\dagger(0)\sqrt{6}, \tag{D17}$$

$$S_z(b) = -1/6 + 2a_5^\dagger(0)/\sqrt{18} + 2a_5(0)/\sqrt{18} + 2n_6(0)/3 + n_5(0)/3 - n_3(0)/3 \tag{D18}$$

and

$$S_-(a,\boldsymbol{\delta}_2) = -a_4^\dagger(\boldsymbol{\delta}_2)/\sqrt{18} + a_6(\boldsymbol{\delta}_2)/\sqrt{6}, \tag{D19}$$

$$S_+(a,\boldsymbol{\delta}_2) = -a_4(\boldsymbol{\delta}_2)/\sqrt{18} + a_6^\dagger(\boldsymbol{\delta}_2)/\sqrt{6}, \tag{D20}$$

$$S_z(a,\boldsymbol{\delta}_2) = \frac{1}{3} - \frac{a_5^\dagger(\boldsymbol{\delta}_2)}{\sqrt{18}} - \frac{a_5(\boldsymbol{\delta}_2)}{\sqrt{18}} - \frac{5n_3(\boldsymbol{\delta}_2)}{6} - \frac{n_4(\boldsymbol{\delta}_2)}{2} - \frac{n_5(\boldsymbol{\delta}_2)}{6} + \frac{n_6(\boldsymbol{\delta}_2)}{6}. \tag{D21}$$

Thus, we obtain the Hamiltonian

$$\mathcal{H} = j[-a_4^\dagger(0)a_4(\boldsymbol{\delta}_2) - 3a_6^\dagger(\boldsymbol{\delta}_2)a_6(0) - a_4^\dagger(\boldsymbol{\delta}_2)a_4(0) - 3a_6^\dagger(0)a_6(\boldsymbol{\delta}_2)]/18 + j[5n_3(\boldsymbol{\delta}_2) + 3n_4(\boldsymbol{\delta}_2) + n_5(\boldsymbol{\delta}_2) - n_6(\boldsymbol{\delta}_2) + 8n_6(0) + 4n_5(0) - 4n_3(0)]/36 + j[-a_5^\dagger(0)a_5(\boldsymbol{\delta}_2) - a_5^\dagger(\boldsymbol{\delta}_2)a_5(0)]/9. \tag{D22}$$

4. b at 0 interacts with c at $\boldsymbol{\delta}_4$

Here,

$$S_-(b) = 2a_4^\dagger(0)/\sqrt{18} - 2a_6(0)/\sqrt{6}, \tag{D23}$$

$$S_+(b) = 2a_4(0)/\sqrt{18} - 2a_6^\dagger(0)/\sqrt{6}, \tag{D24}$$

$$S_z(b) = -1/6 + 2a_5^\dagger(0)/\sqrt{18} + 2a_5(0)/\sqrt{18} + 2n_6(0)/3 + n_5(0)/3 - n_3(0)/3 \tag{D25}$$

and

$$S_-(c,\boldsymbol{\delta}_4) = -a_4^\dagger(\boldsymbol{\delta}_4)/\sqrt{18} + a_6(\boldsymbol{\delta}_4)/\sqrt{6}, \tag{D26}$$

$$S_+(c,\boldsymbol{\delta}_4) = -a_4(\boldsymbol{\delta}_4)/\sqrt{18} + a_6^\dagger(\boldsymbol{\delta}_4)/\sqrt{6}, \tag{D27}$$

$$S_z(c,\boldsymbol{\delta}_4) = \frac{1}{3} - \frac{a_5^\dagger(\boldsymbol{\delta}_4)}{\sqrt{18}} - \frac{a_5(\boldsymbol{\delta}_4)}{\sqrt{18}} - \frac{5n_3(\boldsymbol{\delta}_4)}{6} - \frac{n_4(\boldsymbol{\delta}_4)}{2} - \frac{n_5(\boldsymbol{\delta}_4)}{6} + \frac{n_6(\boldsymbol{\delta}_4)}{6}. \tag{D28}$$

Thus, we obtain the Hamiltonian

$$\mathcal{H} = j[-a_4^\dagger(0)a_4(\boldsymbol{\delta}_4) - 3a_6^\dagger(\boldsymbol{\delta}_4)a_6(0) - a_4^\dagger(\boldsymbol{\delta}_4)a_4(0) - 3a_6^\dagger(0)a_6(\boldsymbol{\delta}_4)]/18 + j[5n_3(\boldsymbol{\delta}_4) + 3n_4(\boldsymbol{\delta}_4) + n_5(\boldsymbol{\delta}_4) - n_6(\boldsymbol{\delta}_4) + 8n_6(0) + 4n_5(0) - 4n_3(0)]/36 + j[-a_5^\dagger(0)a_5(\boldsymbol{\delta}_4) - a_5^\dagger(\boldsymbol{\delta}_4)a_5(0)]/9. \tag{D29}$$

5. c at 0 interacts with a at $\boldsymbol{\delta}_1$ and $\boldsymbol{\delta}_2$

Here,

$$S_-(c) = -a_4^\dagger(0)/\sqrt{18} + a_6(0)/\sqrt{6}, \tag{D30}$$

$$S_+(c) = -a_4(0)/\sqrt{18} + a_6^\dagger(0)/\sqrt{6}, \tag{D31}$$

$$S_z(c) = \frac{1}{3} - \frac{a_5^\dagger(0)}{\sqrt{18}} - \frac{a_5(0)}{\sqrt{18}} + \frac{n_6(0)}{6} - \frac{n_5(0)}{6} - \frac{n_4(0)}{2} - \frac{5n_3(0)}{6} \tag{D32}$$

and, where $\boldsymbol{\delta}$ assumes the values $\boldsymbol{\delta}_1$ and $\boldsymbol{\delta}_2$,

$$S_-(a,\boldsymbol{\delta}) = -a_4^\dagger(\boldsymbol{\delta})/\sqrt{18} + a_6(\boldsymbol{\delta})/\sqrt{6}, \tag{D33}$$

$$S_+(a,\boldsymbol{\delta}) = -a_4(\boldsymbol{\delta})/\sqrt{18} + a_6^\dagger(\boldsymbol{\delta})/\sqrt{6}, \tag{D34}$$

$$S_z(a,\boldsymbol{\delta}) = \frac{1}{3} - \frac{a_5^\dagger(\boldsymbol{\delta})}{\sqrt{18}} - \frac{a_5(\boldsymbol{\delta})}{\sqrt{18}} - \frac{5n_3(\boldsymbol{\delta})}{6} - \frac{n_4(\boldsymbol{\delta})}{2} - \frac{n_5(\boldsymbol{\delta})}{6} + \frac{n_6(\boldsymbol{\delta})}{6}. \tag{D35}$$

Thus,

$$\mathcal{H} = \sum_{\boldsymbol{\delta}} \Big(\frac{k}{36}[a_4^\dagger(0)a_4(\boldsymbol{\delta}) + 3a_6^\dagger(\boldsymbol{\delta})a_6(0) + a_4^\dagger(\boldsymbol{\delta})a_4(0) + 3a_6^\dagger(0)a_6(\boldsymbol{\delta})] + \frac{k}{18}[-5n_3(\boldsymbol{\delta}) - 3n_4(\boldsymbol{\delta}) - n_5(\boldsymbol{\delta}) + n_6(\boldsymbol{\delta}) + n_6(0) - n_5(0) - 3n_4(0) - 5n_3(0)] + \frac{k}{18}[a_5^\dagger(0)a_5(\boldsymbol{\delta}) + a_5(0)a_5^\dagger(\boldsymbol{\delta})] \Big). \tag{D36}$$

6. c at 0 interacts with b at $\boldsymbol{\delta}_1$

Here,

$$S_-(c) = -a_4^\dagger(0)/\sqrt{18} + a_6(0)/\sqrt{6}, \tag{D37}$$

$$S_+(c) = -a_4(0)/\sqrt{18} + a_6^\dagger(0)/\sqrt{6}, \tag{D38}$$

$$S_z(c) = \frac{1}{3} - \frac{a_5^\dagger(0)}{\sqrt{18}} - \frac{a_5(0)}{\sqrt{18}} + \frac{n_6(0)}{6} - \frac{n_5(0)}{6} - \frac{n_4(0)}{2} - \frac{5n_3(0)}{6} \tag{D39}$$

and

$$S_-(b,\boldsymbol{\delta}_1) = 2a_4^\dagger(\boldsymbol{\delta}_1)/\sqrt{18} - 2a_6(\boldsymbol{\delta}_1)/\sqrt{6}, \tag{D40}$$

$$S_+(b,\boldsymbol{\delta}_1) = 2a_4(\boldsymbol{\delta}_1)/\sqrt{18} - 2a_6^\dagger(\boldsymbol{\delta}_1)/\sqrt{6}, \tag{D41}$$

$$S_z(b,\boldsymbol{\delta}_1) = -\frac{1}{6} + \frac{2a_5^\dagger(\boldsymbol{\delta}_1)}{\sqrt{18}} + \frac{2a_5(\boldsymbol{\delta}_1)}{\sqrt{18}} - \frac{n_3(\boldsymbol{\delta}_1)}{3} + \frac{n_5(\boldsymbol{\delta}_1)}{3} + \frac{2n_6(\boldsymbol{\delta}_1)}{3}. \quad \text{(D42)}$$

Thus,

$$\begin{aligned}\mathcal{H} = {} & j[-a_4^\dagger(0)a_4(\boldsymbol{\delta}_1) - 3a_6^\dagger(\boldsymbol{\delta}_1)a_6(0) - a_4^\dagger(\boldsymbol{\delta}_1)a_4(0) \\ & - 3a_6^\dagger(0)a_6(\boldsymbol{\delta}_1)]/18 + j[-4n_3(\boldsymbol{\delta}_1) + 4n_5(\boldsymbol{\delta}_1) + 8n_6(\boldsymbol{\delta}_1) \\ & - n_6(0) + n_5(0) + 3n_4(0) + 5n_3(0)]/36 \\ & + j[-a_5^\dagger(0)a_5(\boldsymbol{\delta}_1) - a_5(0)a_5^\dagger(\boldsymbol{\delta}_1)]/9. \quad \text{(D43)}\end{aligned}$$

7. Summary

Summing all the above contributions, we get the Hamiltonian for the band at energy J for the ferromagnetic configuration as

$$\begin{aligned}V(3J/2) = \sum_{\mathbf{R}} \Big[& 2k[n_6(\mathbf{R}) - n_5(\mathbf{R}) - 3n_4(\mathbf{R}) - 5n_3(\mathbf{R}) \\ & - 5n_3(\mathbf{R}_1) - 3n_4(\mathbf{R}_1) - n_5(\mathbf{R}_1) + n_6(\mathbf{R}_1)]/9 \\ & + j[7n_6(\mathbf{R}) + 5n_5(\mathbf{R}) + 3n_4(\mathbf{R}) + n_3(\mathbf{R}) \\ & + n_3(\mathbf{R}_1) + 3n_4(\mathbf{R}_1) + 5n_5(\mathbf{R}_1) + 7n_6(\mathbf{R}_1)]/18 \\ & + \sum_{\boldsymbol{\delta}} j([-a_4^\dagger(\mathbf{R})a_4(\mathbf{R}+\boldsymbol{\delta}) - a_4^\dagger(\mathbf{R}+\boldsymbol{\delta})a_4(\mathbf{R}) \\ & - 3a_6^\dagger(\mathbf{R})a_6(\mathbf{R}+\boldsymbol{\delta}) - 3a_6^\dagger(\mathbf{R}+\boldsymbol{\delta})a_6(\mathbf{R}) \\ & - 2a_5^\dagger(\mathbf{R})a_5(\mathbf{R}+\boldsymbol{\delta}) - 2a_5^\dagger(\mathbf{R}+\boldsymbol{\delta})a_5(\mathbf{R})]/18 \\ & + k[a_4^\dagger(\mathbf{R})a_4(\mathbf{R}+\boldsymbol{\delta}) + a_4^\dagger(\mathbf{R}+\boldsymbol{\delta})a_4(\mathbf{R}) \\ & + 2a_5^\dagger(\mathbf{R})a_5(\mathbf{R}+\boldsymbol{\delta}) + 2a_5^\dagger(\mathbf{R}+\boldsymbol{\delta})a_5(\mathbf{R})] \\ & + 3a_6^\dagger(\mathbf{R})a_6(\mathbf{R}+\boldsymbol{\delta}) + 3a_6^\dagger(\mathbf{R}+\boldsymbol{\delta})a_6(\mathbf{R})]/36) \Big]. \quad \text{(D44)}\end{aligned}$$

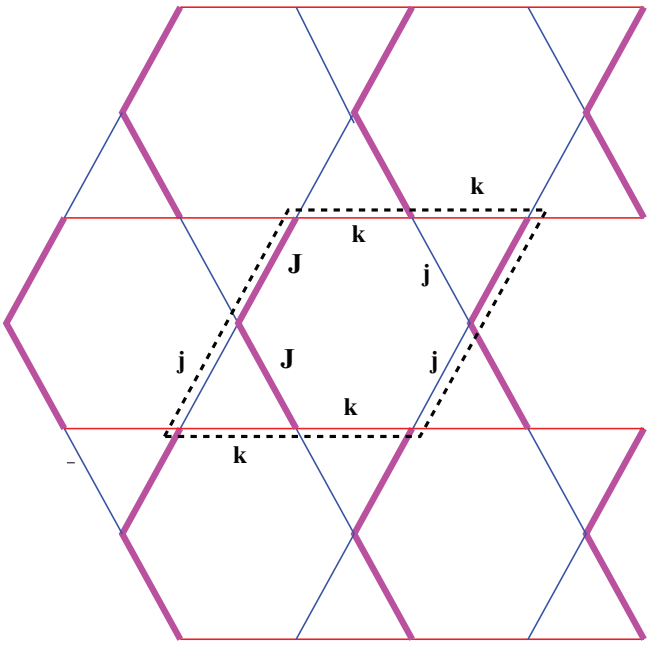

FIG. 10. (Color online) As Fig. 1 for a covering with one trimer per unit cell. In this case, the paramagnetic unit cell contains a single trimer. The magnetic unit cell in the presence of antiferromagnetic trimer ordering is the same as that in Fig. 1 and contains two trimers.

APPENDIX E: ANOTHER TRIMER COVERING

In Fig. 10, we show another covering of the kagome lattice with trimers. If the trimers are antiferromagnetically ordered, then the magnetic unit cell is the same as that of Fig. 1 and one can verify that the spectrum within the ground manifold is again given by Eqs. (8) and (10). However, (as noted by the referee) since this model does not have a screw axis, the degeneracy on the face of the Brillouin zone for the ferromagnetic configuration of trimers will be broken by higher-order corrections.

[1] M. Weinstein, Phys. Rev. D **61**, 034505 (2000).
[2] D. Grohol and D. G. Nocera, Chem. Mater **19**, 3061 (2007).
[3] M. Kohno, O. A. Starykh, and L. Balents, Nat. Phys. **3**, 790 (2007).
[4] M. Ishii, H. Tanaka, M. Hori, H. Uekusa, Y. Ohashi, K. Tatani, Y. Narumi, and K. Kindo, J. Phys. Soc. Jpn. **69**, 340 (2000).
[5] A. Furrer and H. U. Güdel, J. Magn. Magn. Mater. **14**, 256 (1979).
[6] U. Falk, A. Furrer, N. Furer, H. U. Gudel, and J. K. Kjems, Phys. Rev. B **35**, 4893 (1987).
[7] Y. Qiu, C. Broholm, S. Ishiwata, M. Azuma, M. Takano, R. Bewley, and W. J. L. Buyers, Phys. Rev. B **71**, 214439 (2005).
[8] A. Podlesnyak, V. Pomjakushin, E. Pomjakushina, K. Conder, and A. Furrer, Phys. Rev. B **76**, 064420 (2007).
[9] K. Okamoto, T. Tonegawa, Y. Takahashi, and M. Kaburagi, J. Phys.: Condens. Matter **11**, 10485 (1999).
[10] A. Honecker and A. Läuchli, Phys. Rev. B **63**, 174407 (2001).
[11] S.-H. Lee, H. Kikuchi, Y. Qiu, B. Lake, Q. Huang, K. Habicht, and K. Keefer, Nat. Mater. **6**, 853 (2007).
[12] J.-H. Kim, S. Ji, S.-H. Lee, B. Lake, T. Yildirim, H. Nojiri, H. Kikuchi, K. Habicht, Y. Qiu, and K. Kiefer, Phys. Rev. Lett. **101**, 107201 (2008).
[13] A. S. Wills and J.-Y. Henry, J. Phys.: Condens. Matter **20**, 472206 (2008).
[14] A. S. Wills, T. G. Perring, S. Raymond, B. Fäk, J.-Y. Henry, and M. Telling, J. Phys.: Conf. Ser. **145**, 012056 (2009).
[15] The refined crystal structure of $Cu_2(OD)_3Cl$ is given in the Supplementary Information section of Ref. 11.
[16] I. E. Dzialoshinskii, J. Phys. Chem. Solids **4**, 241 (1958).
[17] T. Moriya, Phys. Rev. **120**, 91 (1960).
[18] T. Yildirim and A. B. Harris, Phys. Rev. B **73**, 214446 (2006).

[19]O. Cépas, C. M. Fong, P. W. Leung, and C. Lhuillier, Phys. Rev. B **78**, 140405(R) (2008).

[20]For $j = 0.35$ and $k = 0.46$, the leading-order approximation for the energy gap between the highest-energy J excitation and the lowest-energy $1.5J$ excitation is obtained from Eqs. (28) and (36) to be $1.257 - 1.243 = 0.014$. So, the usefulness of perturbation theory for these values of j and k is problematic.

[21]M. E. Rose, *Elementary Theory of Angular Momentum* (Wiley, New York, 1957).

[22]Note that if one uses the product wave functions of the Néel state, then the phase boundary between ferromagnetic and antiferromagnetic states occurs at $k = j$. For large J, the zero-point corrections to the Néel state phase boundary are more severe than those to the trimer state phase boundary. The effects of such quantum fluctuations on phase boundaries were studied by E. Rastelli and A. B. Harris, Phys. Rev. B **41**, 2449 (1990).

[23]F. Keffer, in *Encyclopedia of Physics: Ferromagnetism*, edited by S. Flügge and H. P. J. Wijn (Springer, Berlin, 1966), p. 1.

[24]V. Heine, *Group Theory in Quantum Mechanics* (Pergamon, New York, 1960), p. 284.

[25]F. J. Dyson, Phys. Rev. **102**, 1217 (1956); **102**, 1230 (1956).

[26]J. desCloizeaux and J. J. Pearson, Phys. Rev. **128**, 2131 (1962).

[27]T. Oguchi, Phys. Rev. **117**, 117 (1959).

[28]For a survey of the structural properties of polymorphs of $Cu_2(OH)_2Cl$, see T. Malcherek and J. Schlüter, Acta Cryst. **B65**, 334 (2009).